Technical Optics with Matter Waves

– geometric, thermal, coherent & quantum

TECHNISCHE UNIVERSITÄT DARMSTADT

M. Sturm
J. Teske
A. Neumann
J. Battenberg
R. Walser

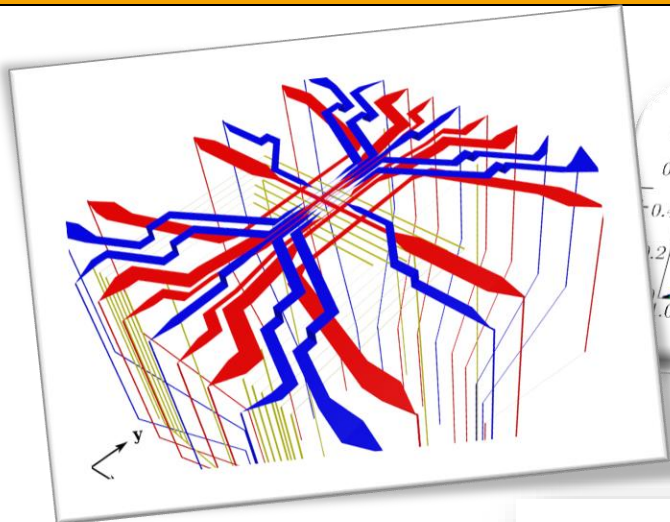

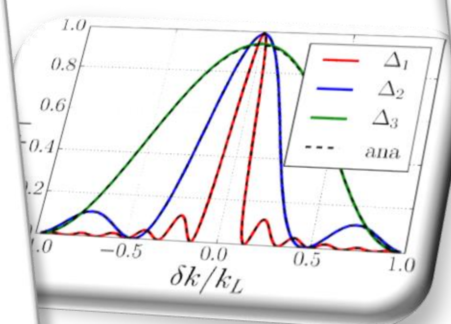

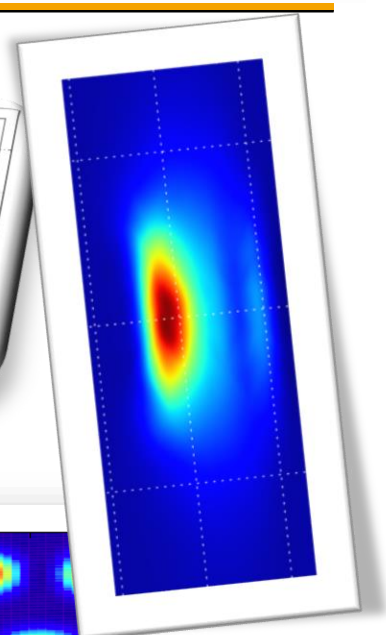

QUANTUS

Collaboration

M. Schlosser
G. Birkl

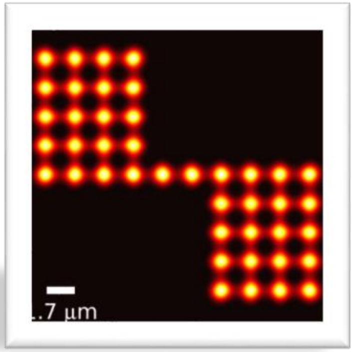

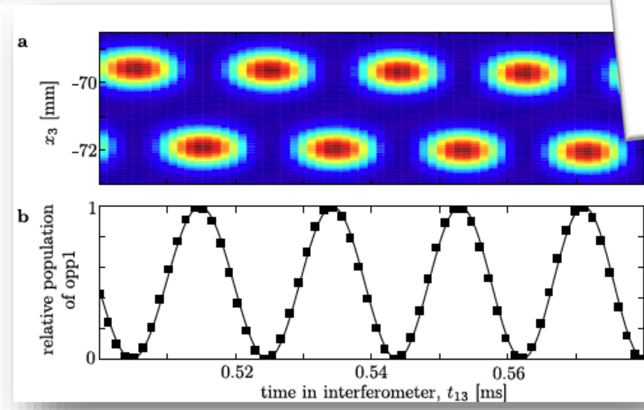

History of success: transistor → IC

TECHNISCHE UNIVERSITÄT DARMSTADT

1947 invention of **transistor,**
J. Bardeen, W. Brattain, W. Shockley @ Bell Labs

1958 invention of **IC Jack Kilby** working at **Texas Instruments**

- Nobelprize 2000 ½
  Z. Alferov ¼ invention of semiconductor heterostructures
- **H. Kroemer** ¼ sc-hs opto-electronics

1970 first handeld battery powered pocket calculator

Canon Pockettronic
using Texas Instruments ICs

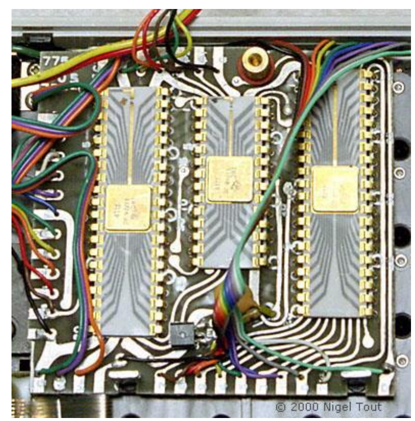

- http://www.ti.com/corp/docs/webemail/2008/enewsltr/public-affairs/graphics/Jack_Kilby300.jpg
- http://www.vintagecalculators.com/assets/images/CanonPocketronic_1.JPG
- http://www.vintagecalculators.com/assets/images/CanonPocketronic_7.jpg

Atomic gas hardware ↔ oxymoron?

TECHNISCHE UNIVERSITÄT DARMSTADT

Either: Experiments q-gases model systems in well controlled lab environments (N>0 students)

Or: quantum technology (EU Flagship program), q-manifesto (T. Calarco)

- **Applications: q-sensing, q-metrology, q-computing**
- **Robustness:** mechanical structures
  - **atomic chips** (J. Schmiedmayer, R. Folman, C. Zimmermann, J. Fortagh, J. Reichel, T. Hänsch, M. Prentiss, P. Treutlein, E. Hinds) lithograyphy, etching

    **Fifteen years of cold matter on the atom chip: promise, realizations, and prospects* *M. Keil et al., JMO, 63, 1840 (2016)*
  - **mirco-lens arrays** (G. Birkl) optical elements, e-beam lithography
  - **3D printing** (H. Giessen, micro-lenses on q-dots)
- **Miniaturization, reproducability, reliability, cost (UHV)**
- **Hybridization: superconductivity, cryo, optical, rf, …**

Cold gases in μ-g

TECHNISCHE UNIVERSITÄT DARMSTADT

University of Hannover

Ernst M. Rasel
Wolfgang Ertmer

ZARM Bremen

Hansjörg Dittus
Claus Lämmerzahl

University of Berlin

Achim Peters

University of Hamburg

Klaus Sengstock

ulm university universität ulm

Wolfgang P. Schleich

Financial support by the

German Space Agency

MPQ Munich and
Laboratoire Kastler Brossel

Theodor W. Hänsch
Jakob Reichel

Ferdinand Braun Institute

A. Wicht

First BEC in space

23.1.2017 BEC MAIUS (S. Seidel) rocket lauched Kiruna, reached 243km, 85 experiments

Lift off at Esrange

Atomic chip

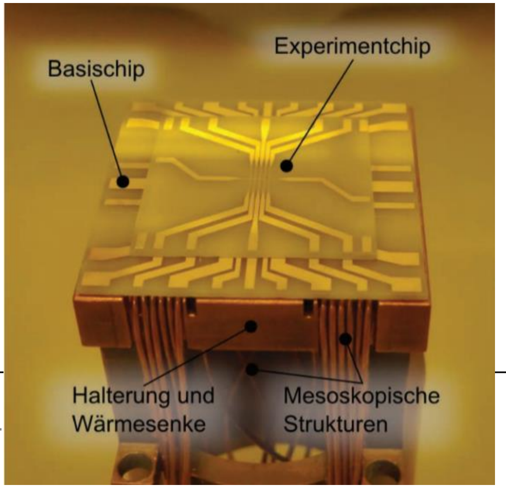

http://www.dlr.de/dlr/en/desktopdefault.aspx/tabid-10081/151_read-20337/#/gallery/25194

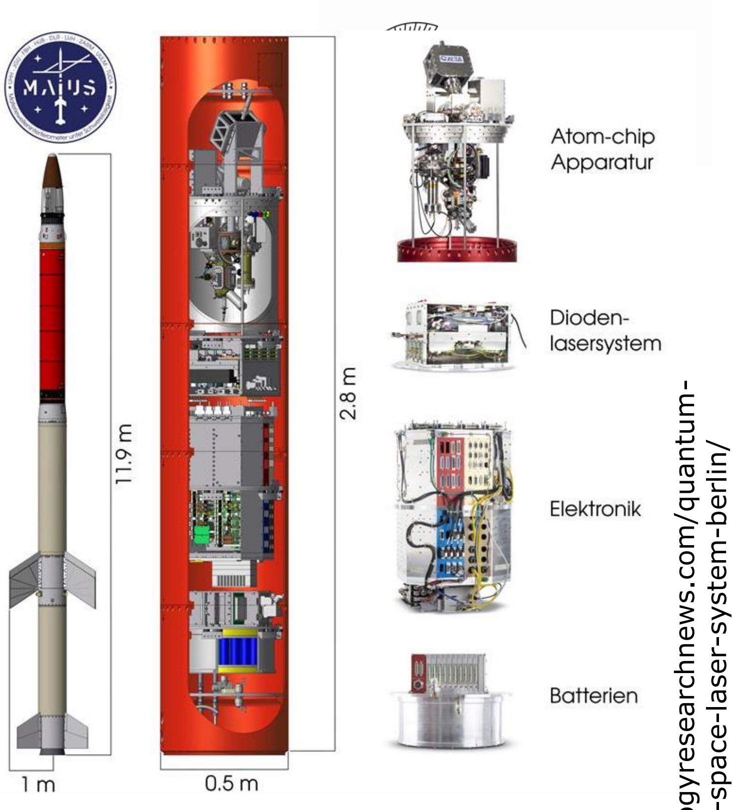

MOPA, HU & Ferdiand-Braun Institute, A. Peters, A. Wicht

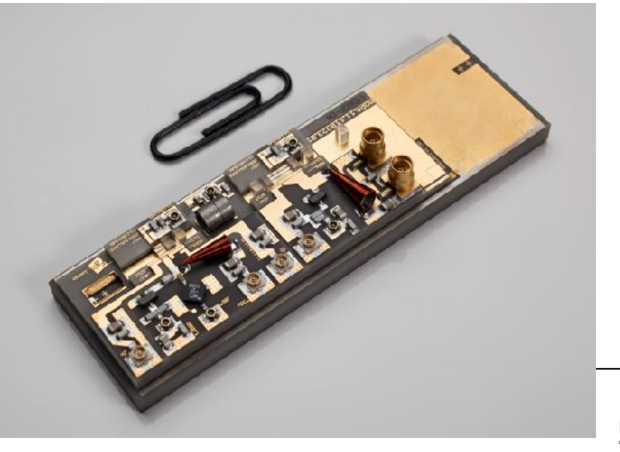

http://www.scienceandtechnologyresearchnews.com/quantum-optical-sensor-first-time-tested-space-laser-system-berlin/

Simulation of mw-devices

- **Challenges:** 3D (dimension), large expansion times (t>2000ms), and scales (d>mm), T(emperature) , $\hbar$ (particle vs. waves), g (nonlinearity), (z^3) anharmonicity, time-dependence (dkc), noise

arXiv:1701.06789, G. Nandi et al., PRA, 76, 063617 (2007)

- **Toolbox mw-optics**
  a. Magnetic traps & lenses
  b. Designing quantum simulators with micro-lens arrays (M. Sturm, M. Schlosser, G. Birkl)
  c. Bragg beam-splitters
- **Methods & applications**
  a. Geometical mw-optics: raytracing, aberrations
  b. Thermal mw-optics: 3D interferometry @ finite T
  c. Coherent mw-optics: delta-kick-collimation
  d. Quantum mw-optics: Josephson-Junction rings

mw-traps & lenses with magnetic chips

J. Battenberg

TECHNISCHE UNIVERSITÄT DARMSTADT

- geom. representation of 2D conducting strips
- Biot-Savart law

$$\mathbf{B}(\mathbf{R}) = \frac{\mu_0 I}{4\pi} \int_C \frac{d\mathbf{l} \times \mathbf{r}}{r^3}$$

$$V(\mathbf{R}) \propto |\mathbf{B}(\mathbf{R}) + \mathbf{B}_{\text{ext}}(\mathbf{R})|$$

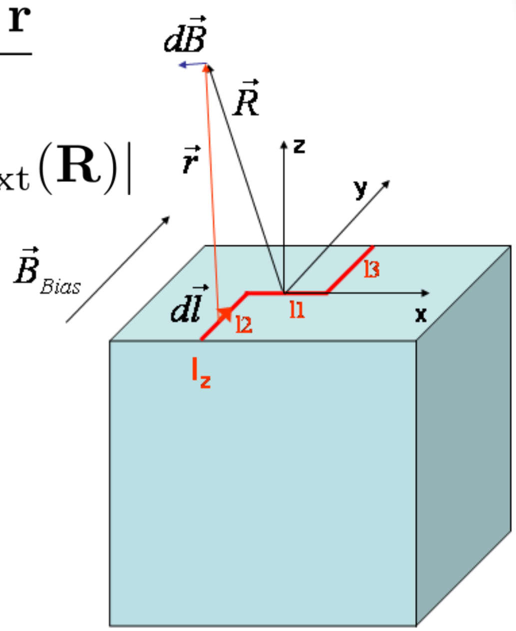

- several active layers
- multi-dimensional current control

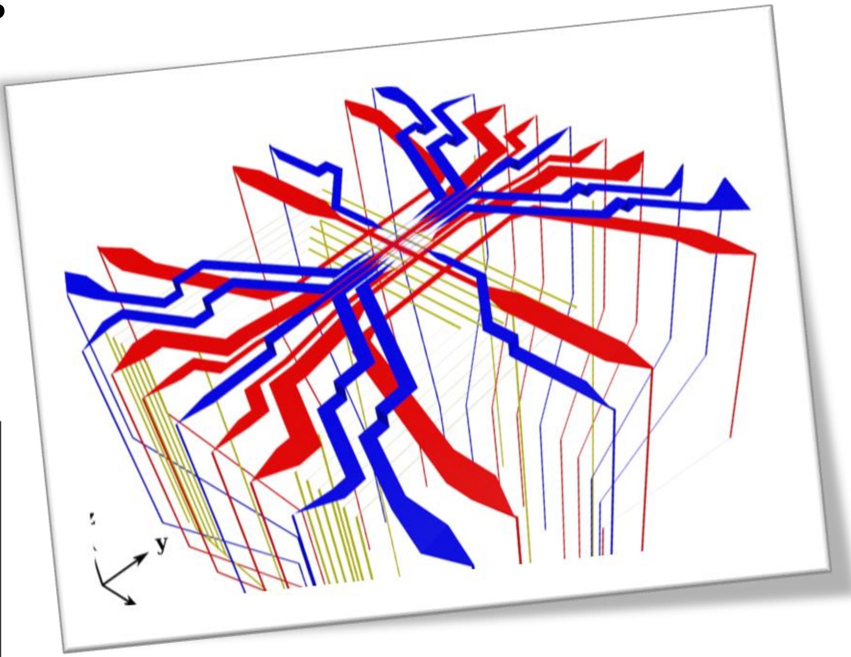

exp. chip design
W. Herr, LHU

Shape of magnetic potential

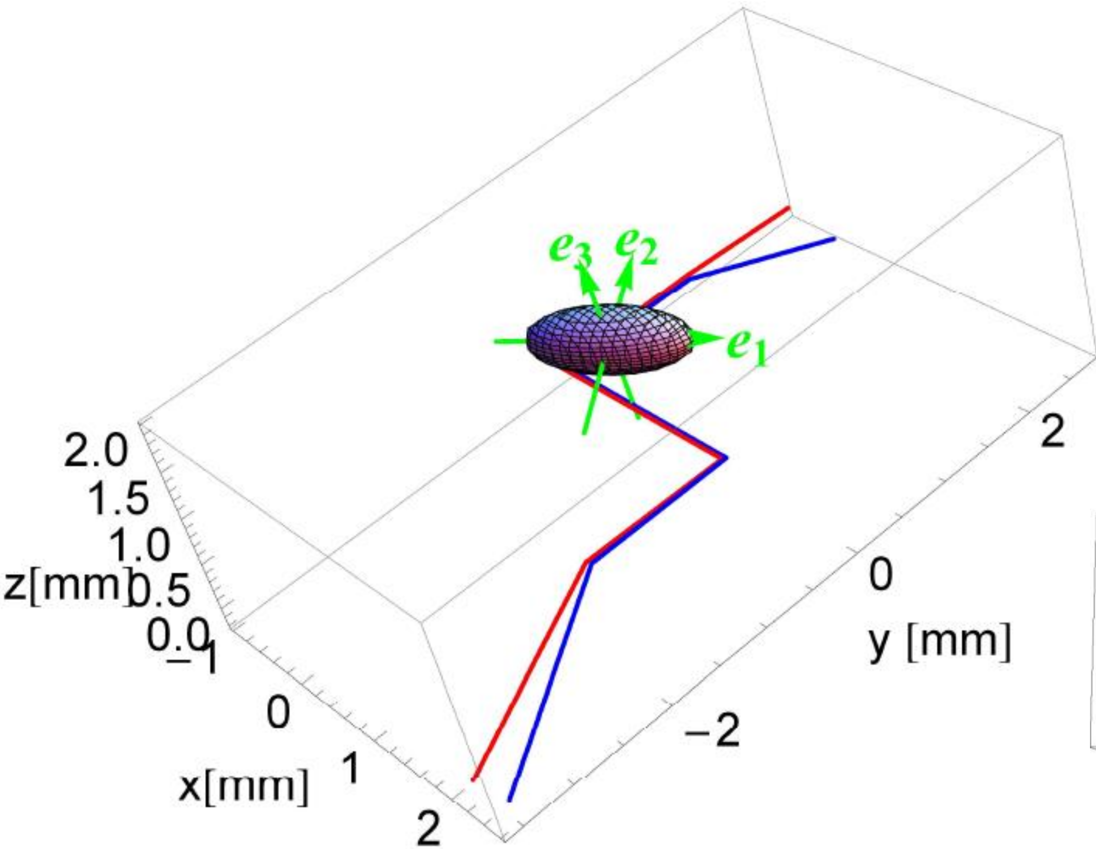

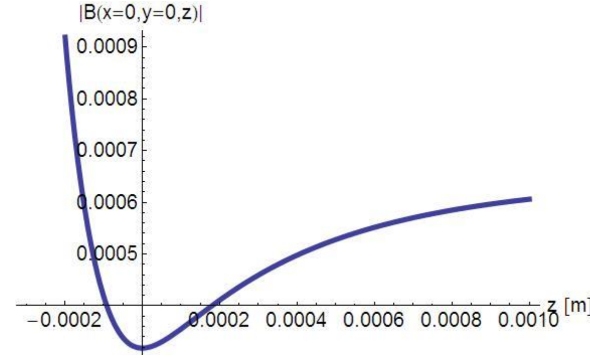

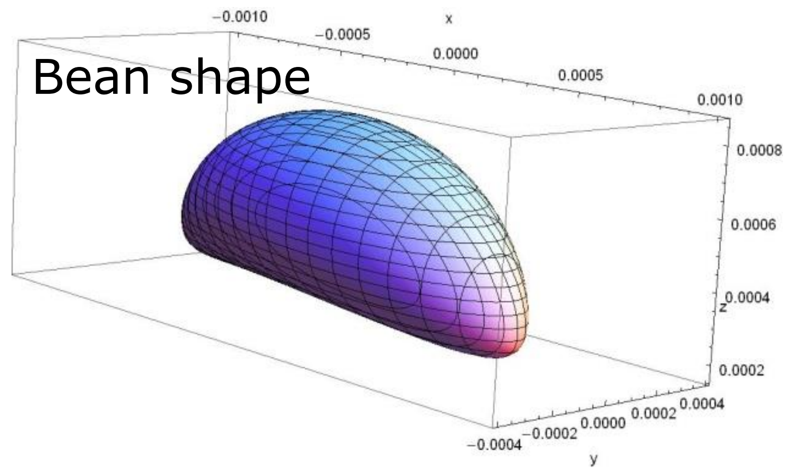

QII frequency manifold

$$\{(\nu_1, \nu_2, \nu_3) \in R^3 | (I_x, I_y, I_b, I_s) \in R^4 \text{ with feasable solution}\}$$

Eigen-frequencies of potential Hess-matrix at potential minimum

Feasible frequencies
2D planar manifold
Earnshaw theorem
magnetic shield

$$\mathbf{B}(\mathbf{R}) = -\nabla \phi_M$$

$$\Delta \phi_M = 0$$

$$\phi_M(\mathbf{r}) = \sum_{lm} \phi_{lm} R_{lm}(\mathbf{r})$$

Map of possible frequencies is current QII setup

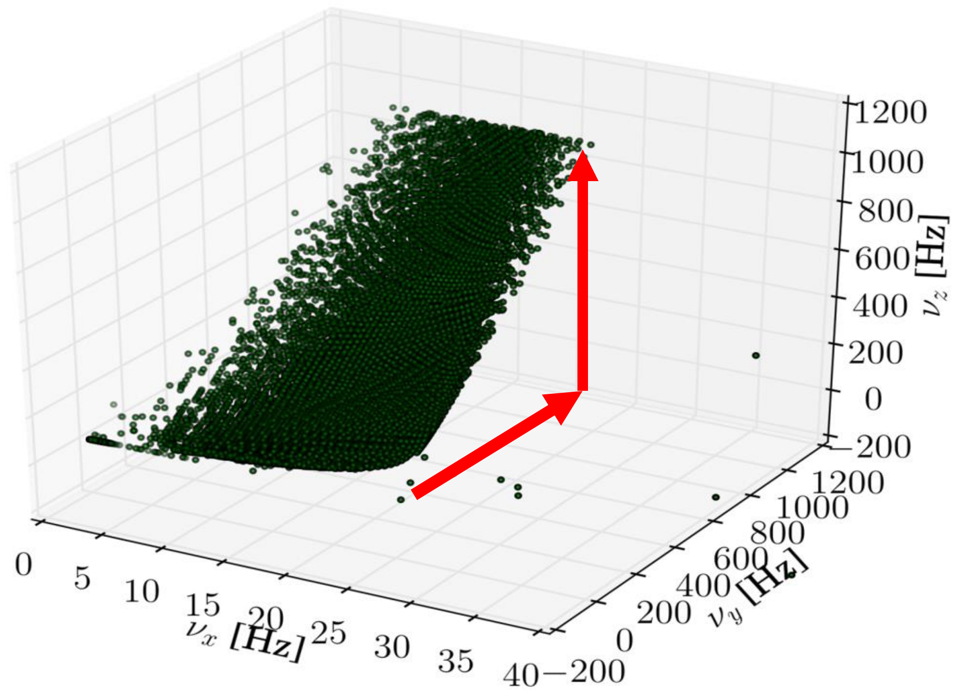

Adjustable optical microtraps arrays

Designing robust light fields in the itinerant tunneling regime

M. Sturm, M. Schlosser, G. Birkl

TECHNISCHE UNIVERSITÄT DARMSTADT

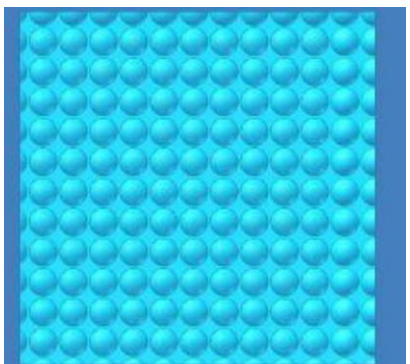

Suss MicroOptics

Microlens arrays with spatial light modulators: arbitrary arrays of microtraps

Quantum simulators by design –many-body physics in reconfigurable arrays of tunnel-coupled traps

arxiv:1705.01271

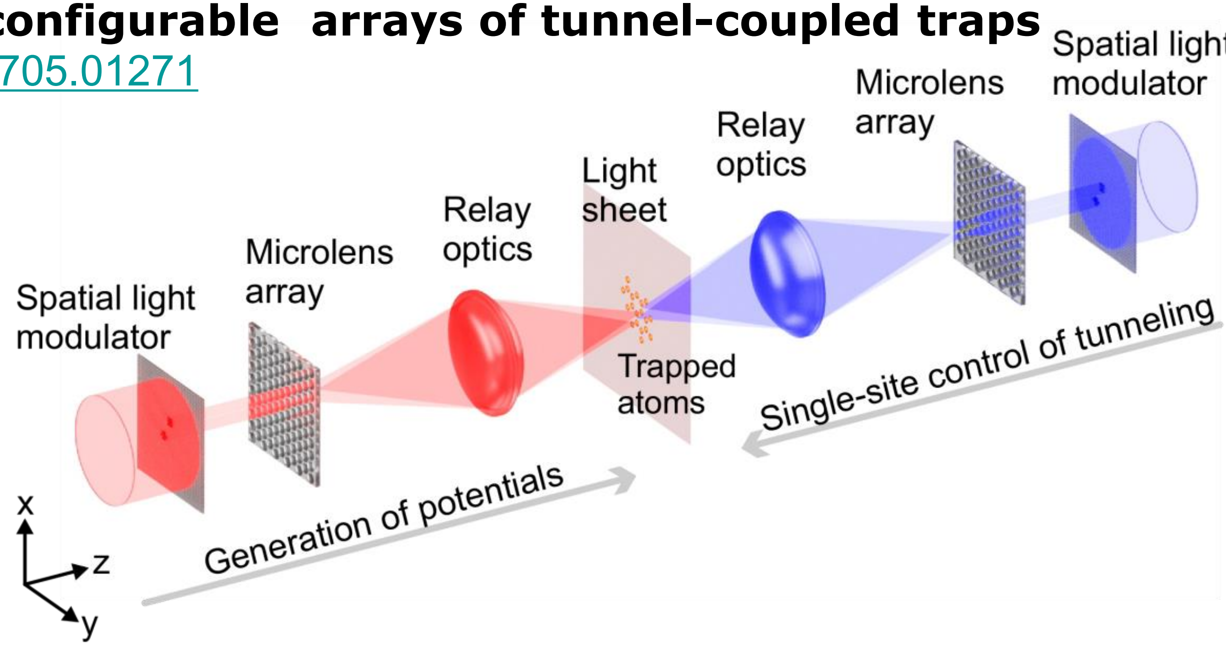

Configurations with tunneling

- **Pinboard for atomtronics**
  implement atomtronic devices
  like diodes and transistors

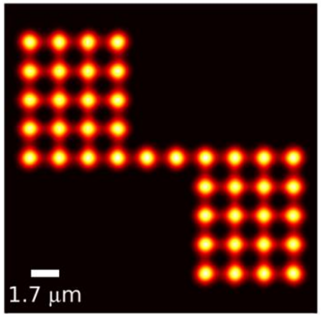

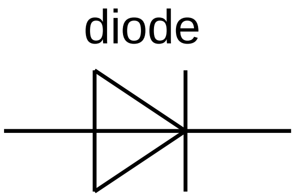

- **Designable lattices**
  Exotic lattice geometries
  quasi crystals
  point/line defects
  controllable disorder

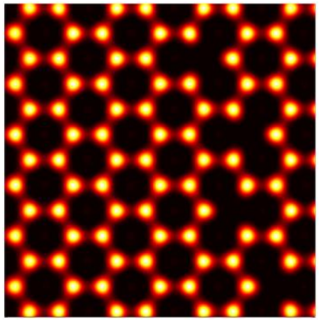

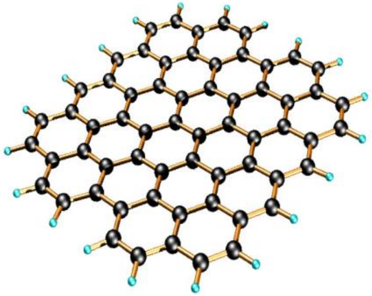

Copyright: Chris Ewels

- **Molecular structures**
  mimick electronic sturcture
  of molecules

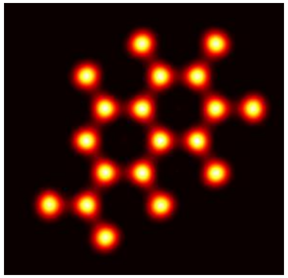

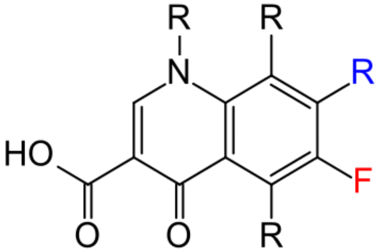

https://en.wikipedia.org/wiki/Quinolone

Simulation of the light field

TECHNISCHE UNIVERSITÄT DARMSTADT

- **Precise optical modeling** using commercial software
- **Microlens array**
  diameter of lenslets: 106 µm
  ~ 100x100 lenslets
  ROC=2.65 mm
- Aspheric lens with NA=0.68
- Raytracing and wave optics

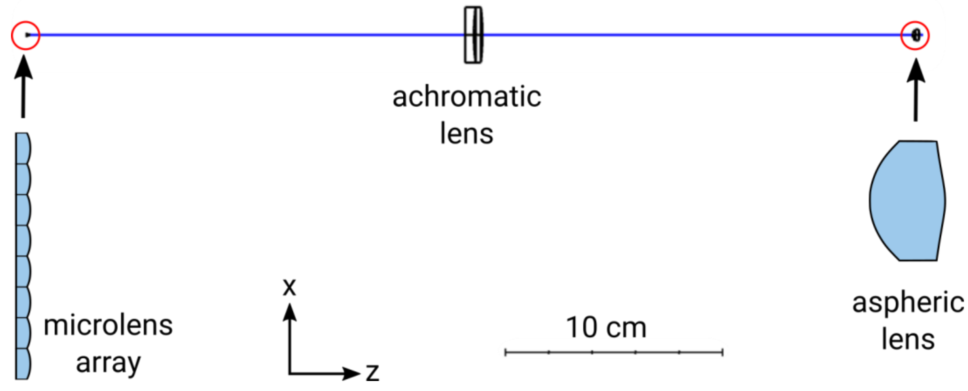

Spot size diagram

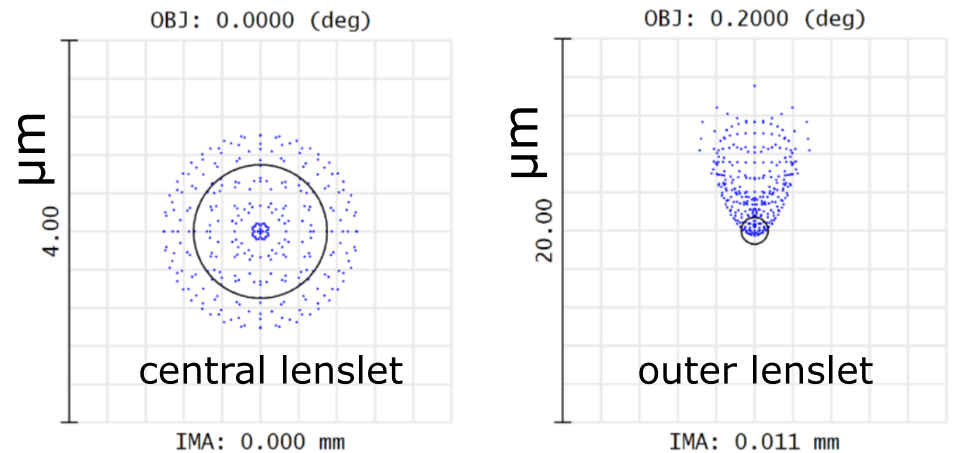

2D Optical potential +1D light sheet

✓ **Measured and simulated** intensity distriubtions agree

$$V(x,y,z) \approx V_\perp(x,y) + V_\parallel(z)$$

$$V_\perp(x,y) = -\sum_{\mathbf{R}_i} V_{0\perp}^{(i)} e^{-2\frac{(x-X_i)^2+(y-Y_i)^2}{w_{0\perp}^2}}$$

$$V_\parallel(z) = -V_{0\parallel} e^{-2z^2/w_{0\parallel}}$$

$d = 1.7\ \mu m \quad w_{0\perp} = 0.7\ \mu m \quad w_{0\parallel} = 2.5\ \mu m$

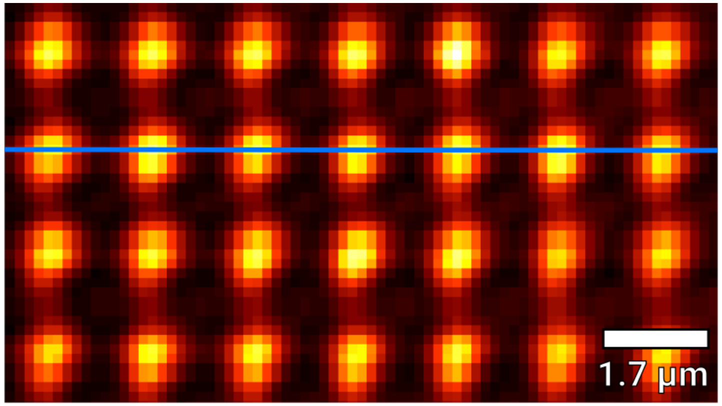

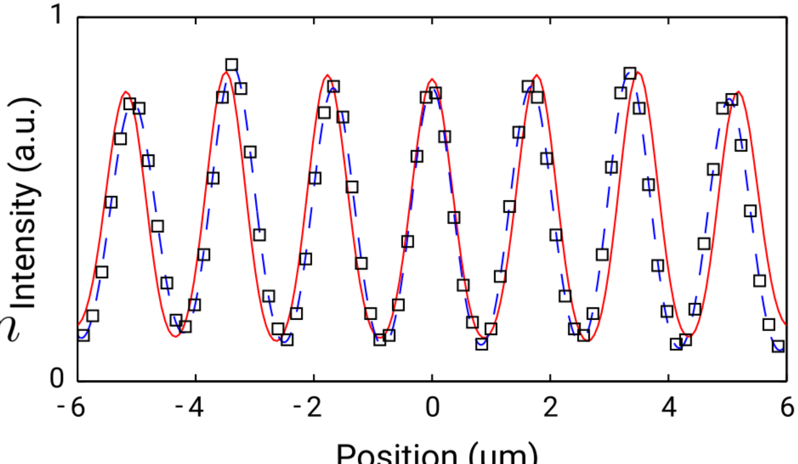

Measurement, Gaussian fit, simulation

Bose-Hubbard parameters

TECHNISCHE UNIVERSITÄT DARMSTADT

- Bose-Hubbard model using 2+1D Schrödinger equation

$$\hat{H} = U \sum_i \hat{a}_i^\dagger \hat{a}_i^\dagger \hat{a}_i \hat{a}_i - J \sum_{\langle ij \rangle} \hat{a}_i^\dagger \hat{a}_j$$

- Onsite interaction

$$U = \frac{4\pi a_s \hbar^2}{m} \int \varphi_i^4(x,y)\phi^4(z)\, d^3r$$

- Nearest-neighbour tunneling

$$J = \langle \varphi_i \phi | \hat{H}_1 | \varphi_j \phi \rangle$$

	Li 7	Na 23	K 41	Rb 87
J/h	18.6 Hz	3.5 Hz	2.3 Hz	1.5 Hz
U/h	186 Hz	35 Hz	23 Hz	15 Hz

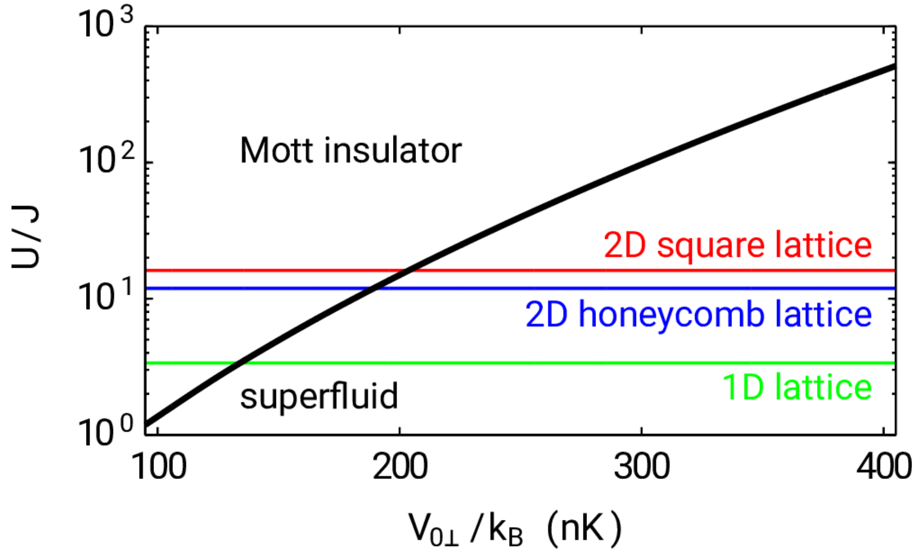

For Rubidium 87

mw-beam splitter

Velocity dispersion of optical Bragg beamspitter in 3D with temporal pulses, spatial beams shapes, wavefront curvature

A. Neumann

TECHNISCHE UNIVERSITÄT DARMSTADT

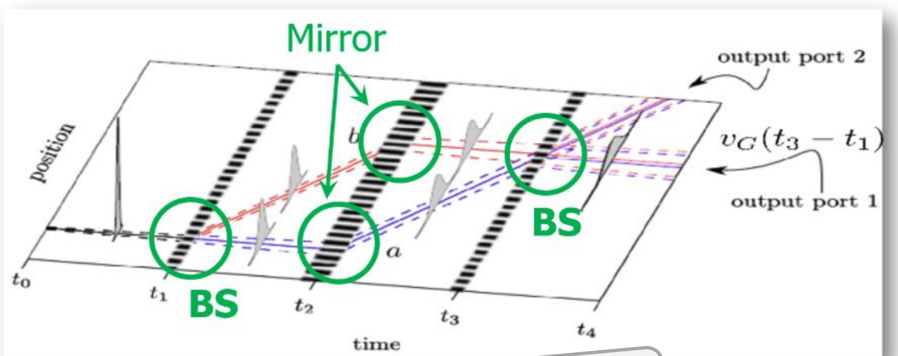

light-matter interaction

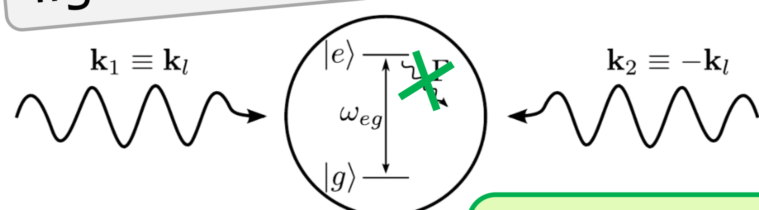

$$\omega_1 = \omega_2 \equiv \omega_l$$
$$\Delta = \omega_{eg} - \omega_l$$

large detuning:
$\Delta = \omega_{eg} - \omega_l, \ |\Delta| \gg \Gamma$

BS goal:
coherently splitting motion of atoms with unit response and wide momentum range

BS: Bragg diffraction of atoms by periodic grating (optical standing wave)

$$\rightarrow \ i\hbar\partial_t|\Psi\rangle = \hat{H}|\Psi\rangle$$

solve with split operator method

Plane wave Bragg diffraction

$$\hat{H} = \frac{\hat{p}^2}{2M} \otimes \mathbb{1} + \frac{\hbar\Delta}{2}\hat{\sigma}_z + \frac{\hbar\Omega_0}{2}$$

$$\Psi(t) = e^{-i\hat{H}t}|\Psi(0)\rangle = \hat{U}|\Psi(0)\rangle$$

Loss into off resonant higher diffraction orders:

$$|\Psi(t)\rangle = \sum_{m=-N}^{N} g_m|g, m \cdot k_l\rangle + e_{m'}|e, m' \cdot k_l\rangle$$

m odd, m' even

absorb / emit 1 photon:

$$e^{\pm i k_l \hat{x}} = \int dp|p \pm \hbar k_l\rangle\langle p|$$

→ coupling:

$$|g, k\rangle \leftrightarrow |g, k \pm 2Nk_l\rangle$$

(Bragg order N)

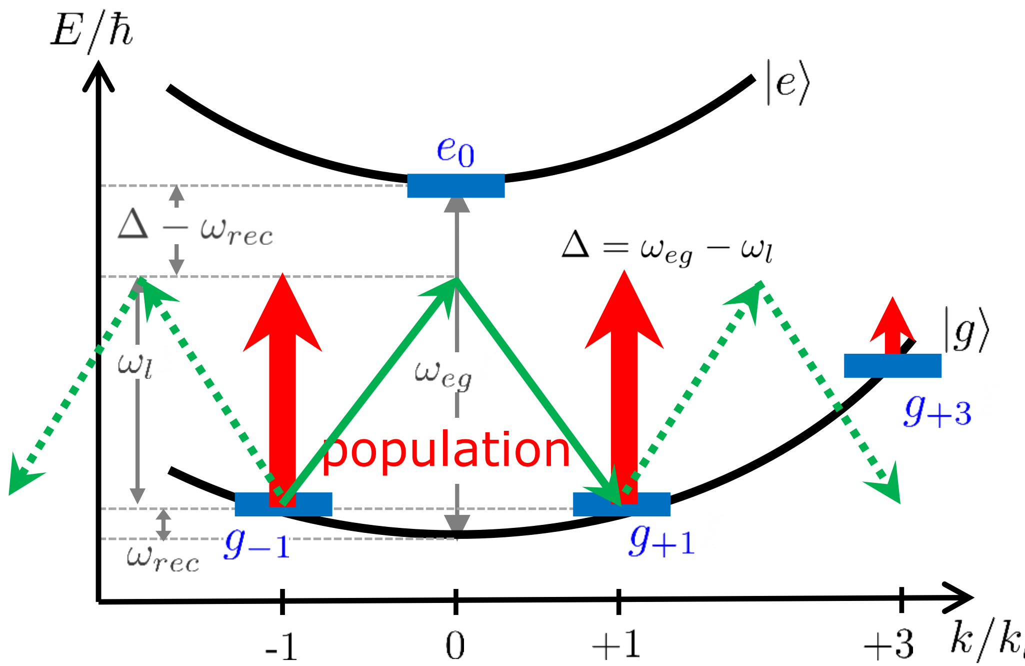

Temporal envelopes

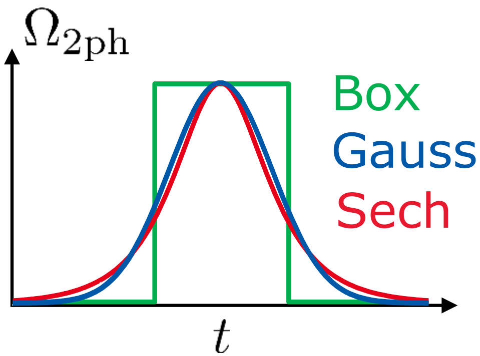

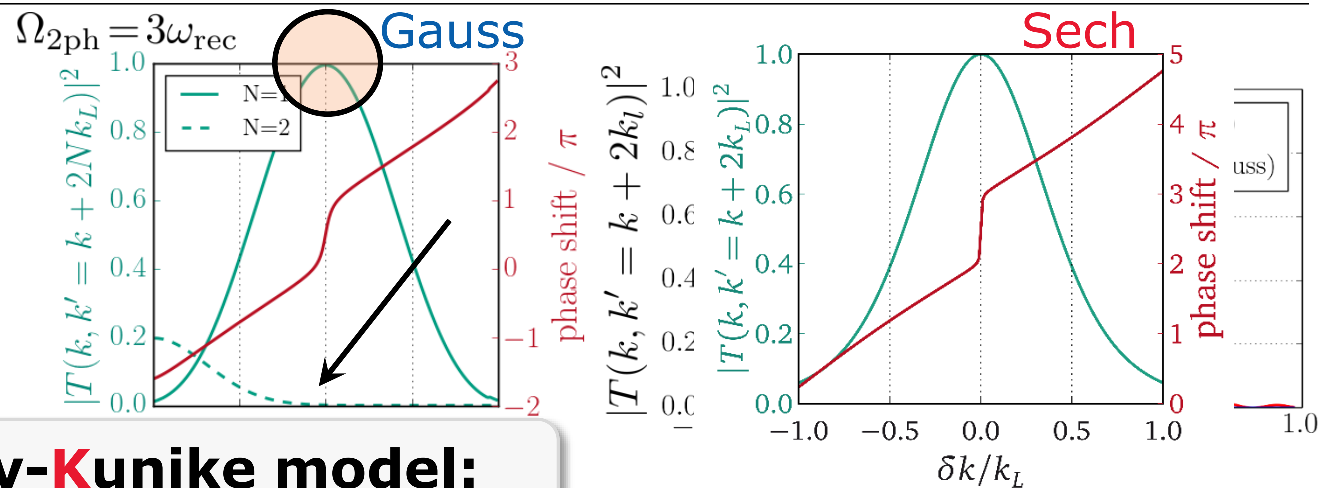

Analytic Demkov-Kunike model:
1D 1st order Bragg diffraction

$$\Omega_{2ph}(t) = \Omega_{2ph} \cdot \mathrm{sech}\left(\sqrt{\frac{\pi}{2}}\frac{t}{\sigma}\right)$$

$$T_{kk'}^{N=1} = \frac{\sigma \Omega_{2ph} \sqrt{\mathrm{sech}\left(\sqrt{\frac{\pi}{2}}\frac{t}{\sigma}\right)}}{i\sqrt{2\pi} - 8\omega_{rec}\delta k \sigma} \cdot {}_2F_1[a, b; c, z(t)]$$

$$a/b = 1 -/+ \frac{\sigma\Omega_{2ph}}{\sqrt{2\pi}}, \quad c = \frac{3}{2} + 2i\sqrt{\frac{2}{\pi}}\omega_{rec}\delta k \sigma, \quad z(t) = \frac{1}{2} + \frac{\tanh\left(\sqrt{\frac{\pi}{2}}\frac{t}{\sigma}\right)}{2}$$

- ✓ suppressed side maxima
- ✓ insignificant population loss into higher diffraction orders
- ✓ Analytic model (DK) for 'sech'- pulses

Comparison of 1D simulation with experimental data*

* M.Gebbe (Universität Bremen, priv. com.)

Laser:
- spatial dependence: ~ plane waves
- temporal: Gaussian (+ fit with **D**emkov **K**unike)
- Laser frequency detuned to resonance Δf_l

Atoms: BEC @ 50 nK ~ Thomas Fermi (width in momentum space $\ll k_l$)

$\Omega_{2ph} \approx 2.5\omega_{rec}$

$t = 200\mu s$ $(t > t_{mirror})$

$\Delta f_l \approx 0$ kHz

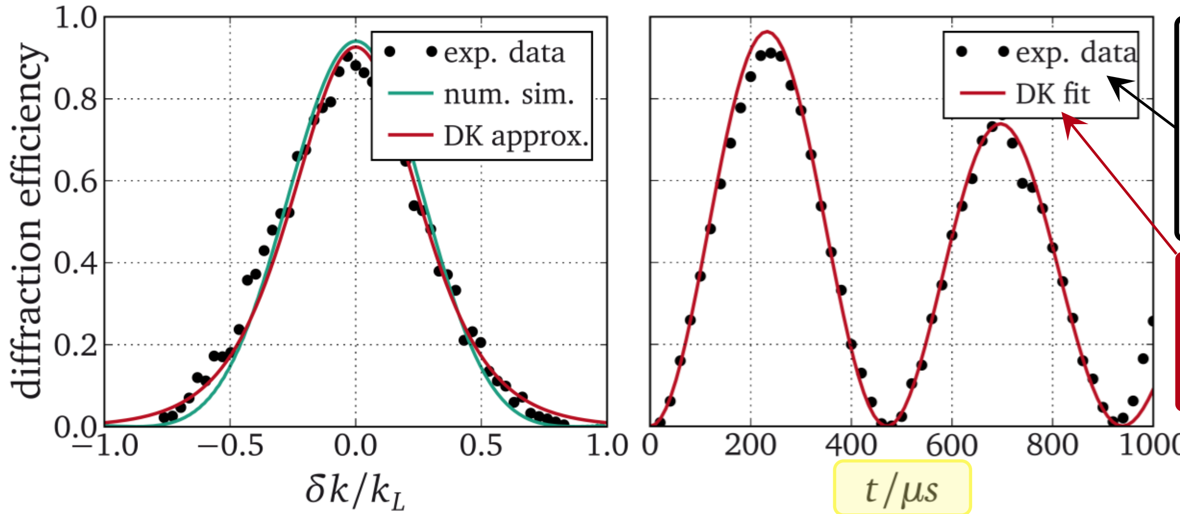

$\Omega_{2ph} \lesssim 2\omega_{rec}$

$\Delta f_l \approx 0$ kHz $(< 2.5$ kHz$)$

$\Omega_{2ph} = 1.8\omega_{rec}$

$\Delta f_l \approx 0.9$ kHz

✓ simulation + DK-approximation match experimental data

Application 1: delta-kick collimation

-geometric-, thermal-, coherent mw optics

B. Okhrimenko, J. Teske

TECHNISCHE UNIVERSITÄT DARMSTADT

Ray optics with light (2+1D) Matter wave optics (3+1D)

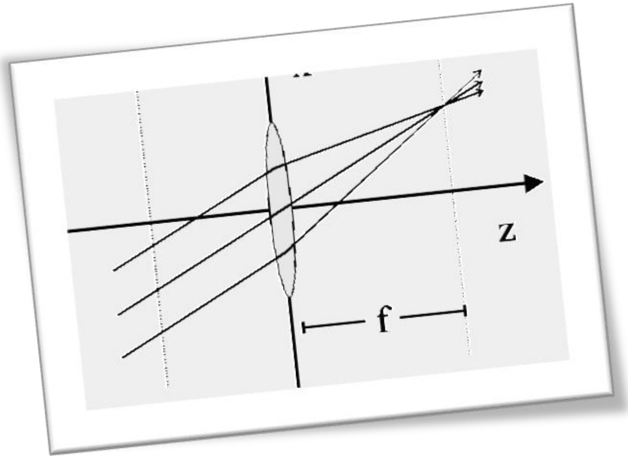

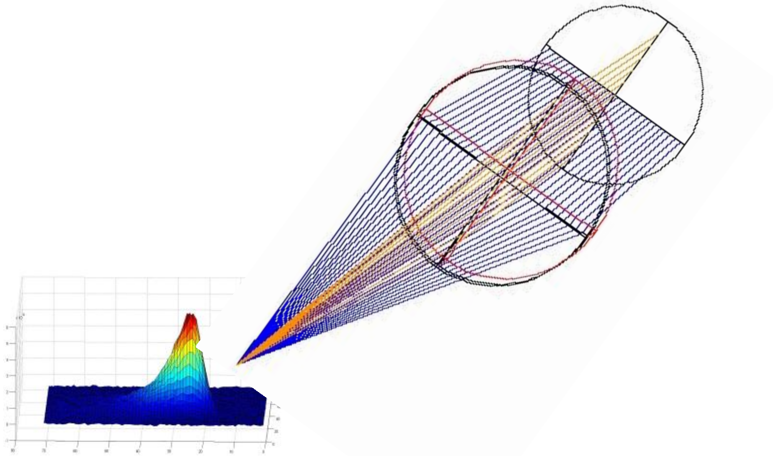

AMMANN, Hubert ; CHRISTENSEN, Nelson: Delta Kick Cooling: A New Method for Cooling Atoms, *Phys. Rev. Lett.* 78, 2088 (1997)

Matter wave optics DKC-sequence:

$$t_{lens} = \frac{1}{\omega}\tan\left(\frac{1}{\omega t_1}\right)$$

DKC of thermal cloud: position

TECHNISCHE UNIVERSITÄT DARMSTADT

DKC sequence:

t_{preToF}= 80 ms,

t_{lens}= 2.64 ms,

t_{ToF}= 200 ms

Pilot rays: estimating final position and width provides integration grid

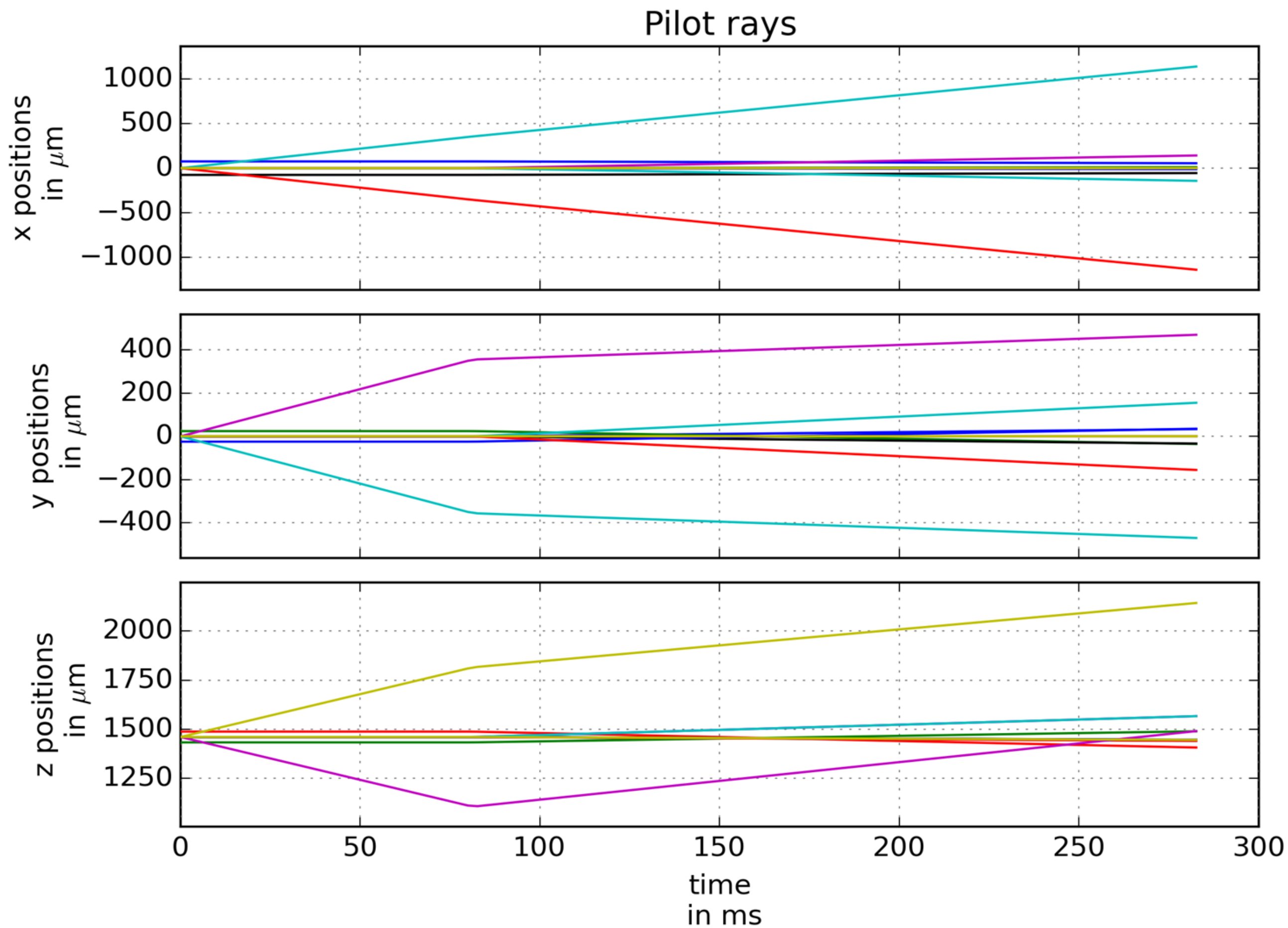

DKC of thermal cloud: velocity

Velocity rays

measure

quality of

collimation

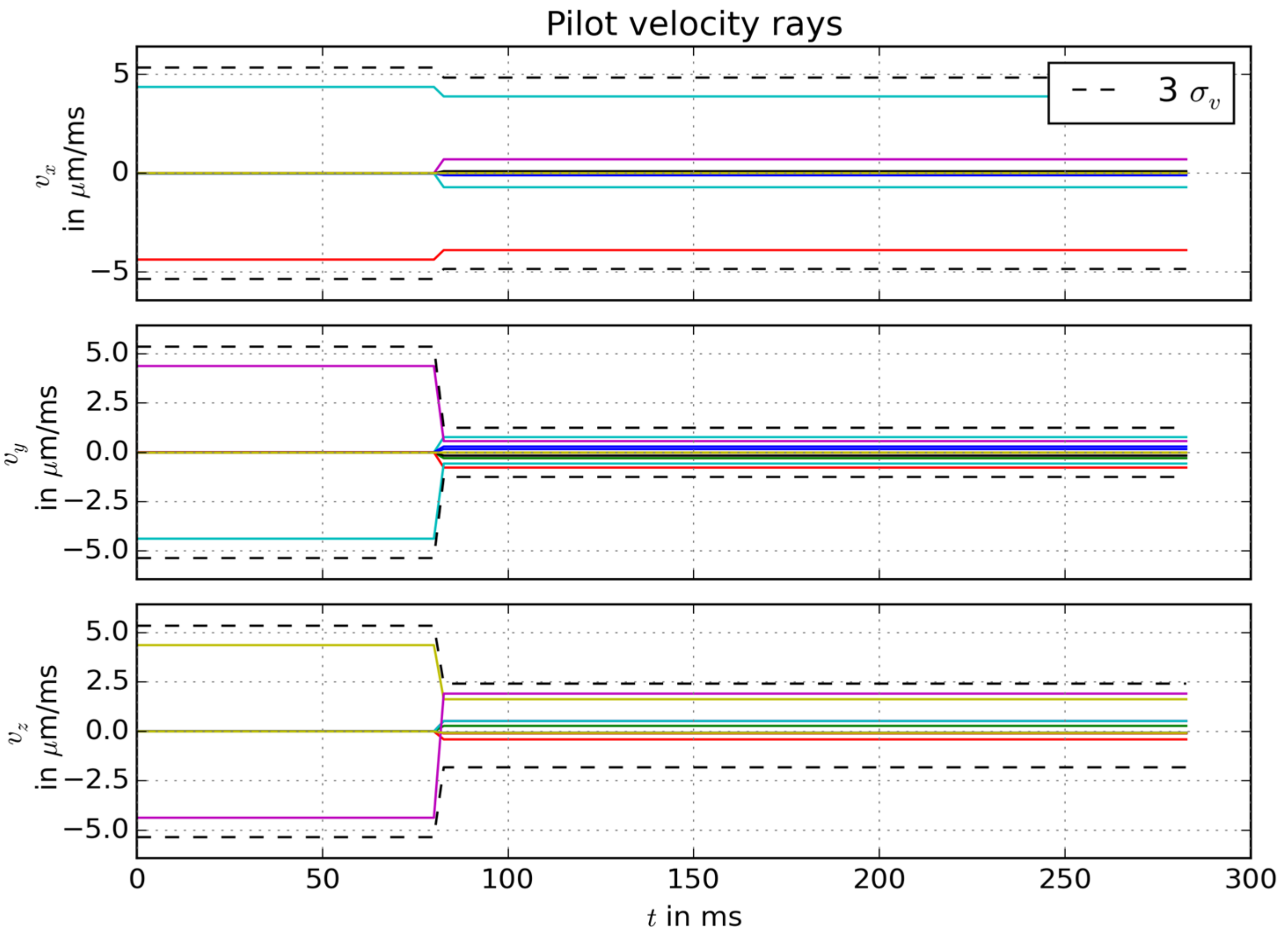

Iso-potential of release trap

I_{BCOz}=6A, I_{SCOz}=2A

I_x=0.1A, I_y=-0.3743A, I_z=0 A

f_1= 9.209 Hz, f_2= 28.479 Hz, f_3= 25.301 Hz

R_{min}=(-1.48e-04, -2.03e-05, 1459.77) µm

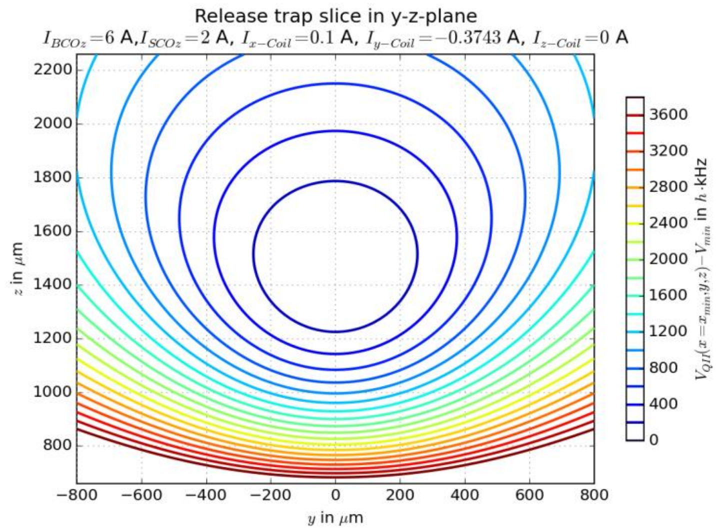

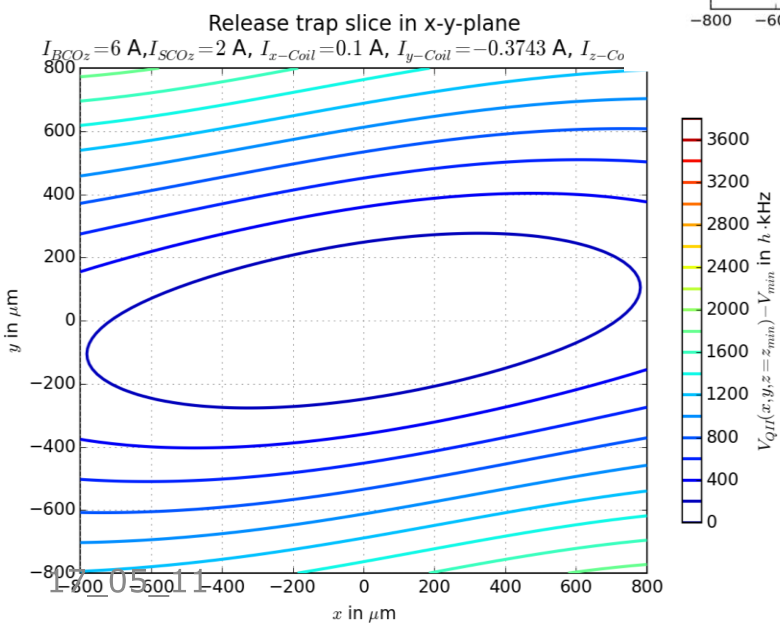

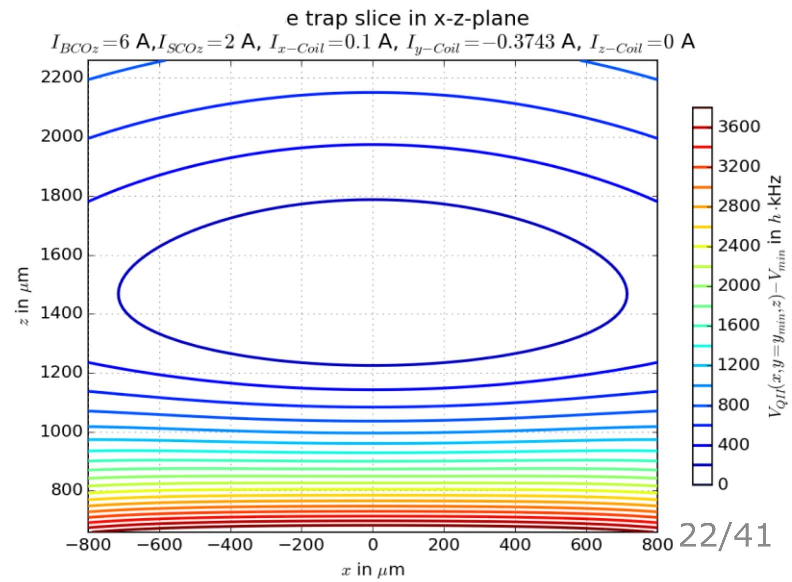

Initial position density $n^{(2)}(y, z, t = 0)$

Initial thermal Wigner distribution: N=10^5 particles, T=100nK (harmonic approximation)

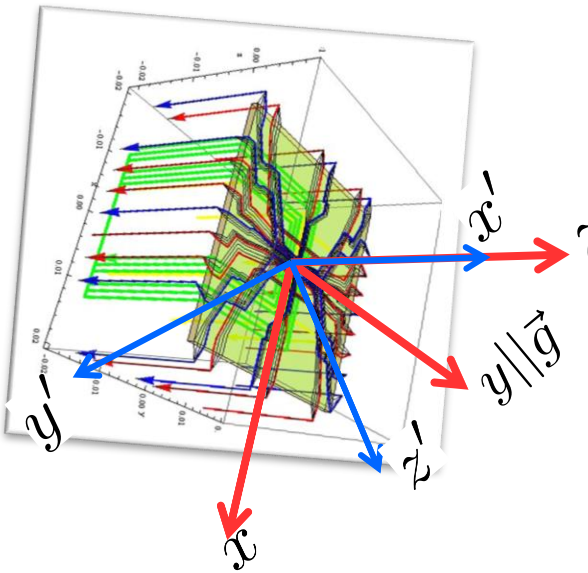

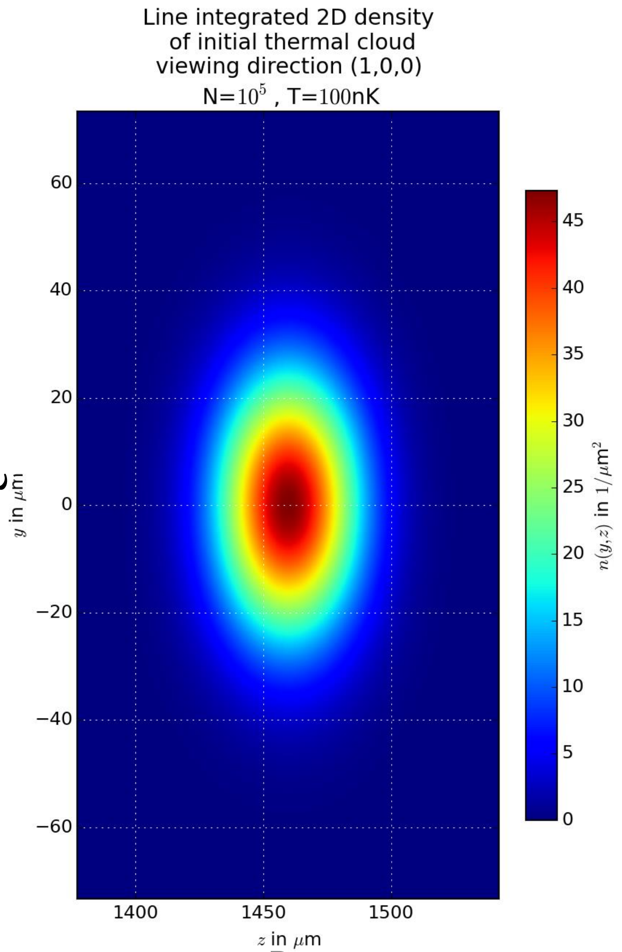

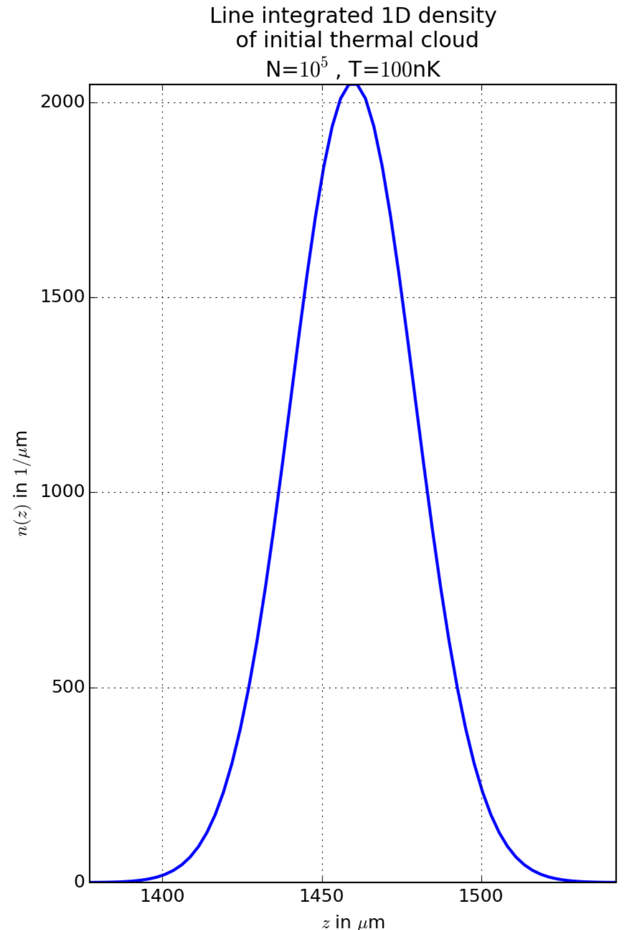

Isopotential of DKC lense

- **Lense kick** t=2.64 ms
- **Anharmonicity**

  deforms gaussian cloud

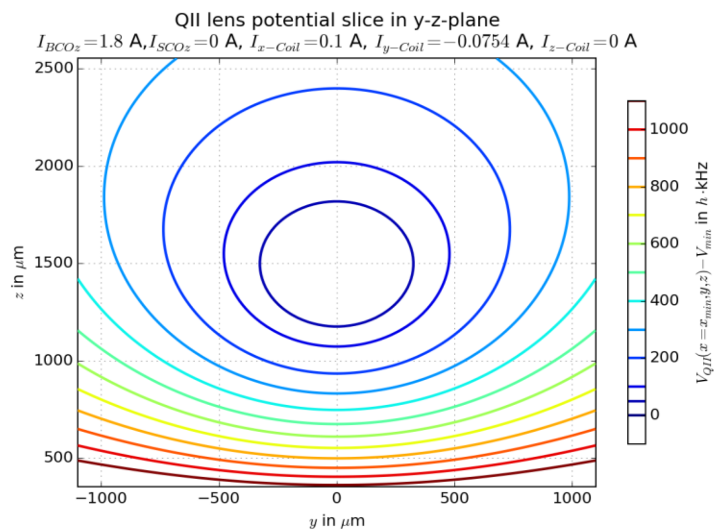

I_{BCOz}=1.8 A, I_{SCOz}=0 A

I_x=0.1A, I_y=-0.0754283 A, I_z=0 A

f_1= 2.961 Hz, f_2= 11.039 Hz, f_3= 11.041 Hz

R_{min}=(-1.2e-03, -1.3e-03, 1453.92) μm

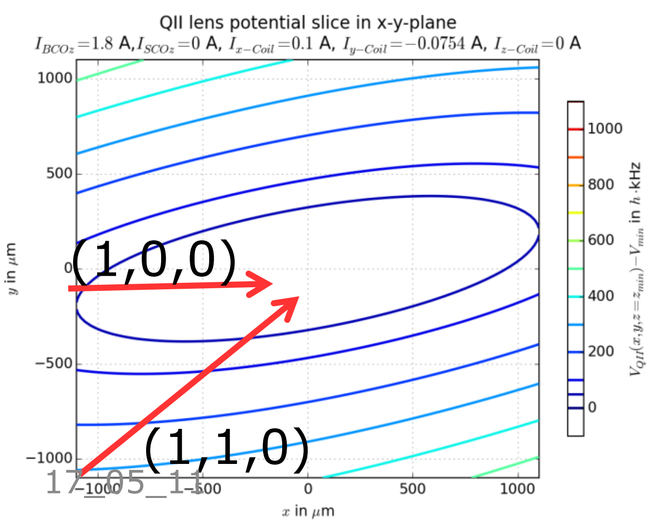

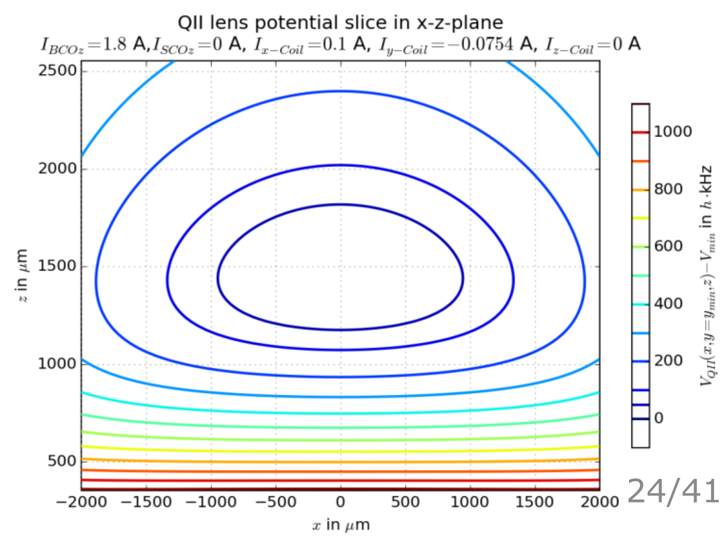

Thermal density $n^{(2)}(y, z, t_f)$

TECHNISCHE UNIVERSITÄT DARMSTADT

t_{ToF}= 200 ms

T=100nK, N=10^5

Axis of sight

(1,1,0) vs. (1,0,0)

Change of 2D shape

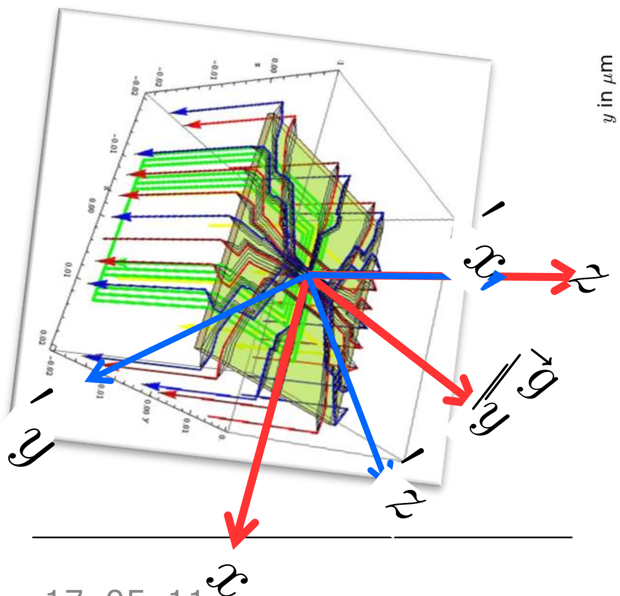

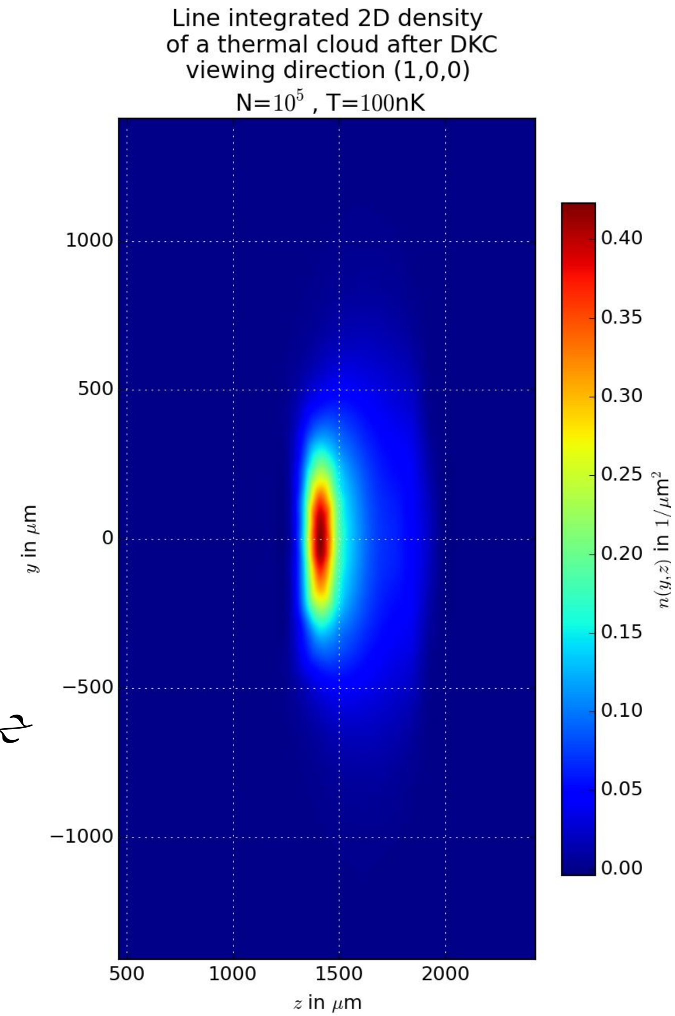

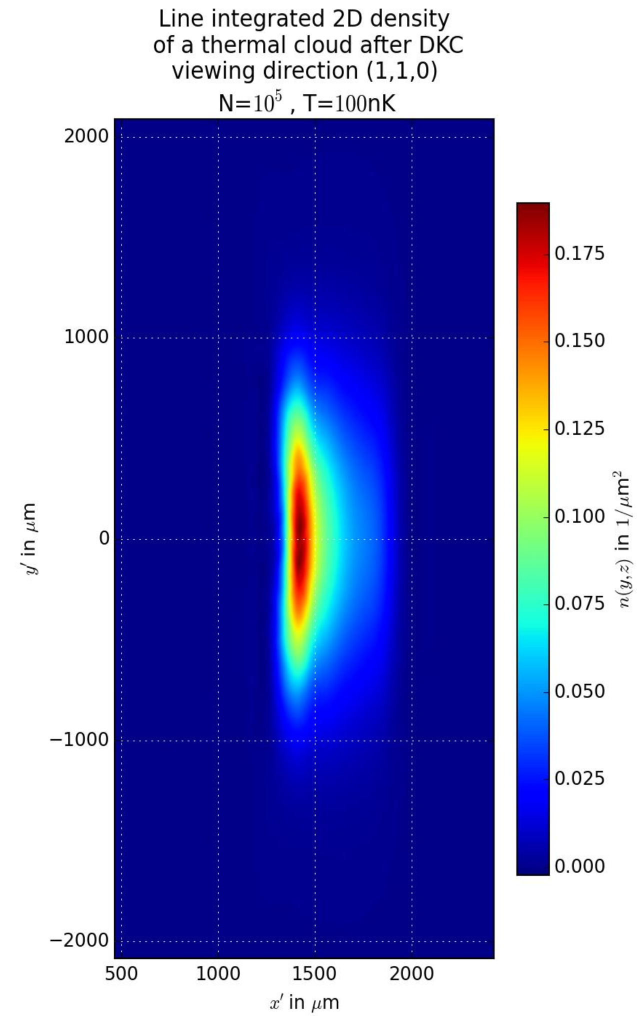

Thermal densisty $n^{(2)}(y,z,t_f)$

t_{ToF}= 200 ms

T=300 nK, N=10^5

Higher temperatures,

higher expansion rates

more unharmonicity

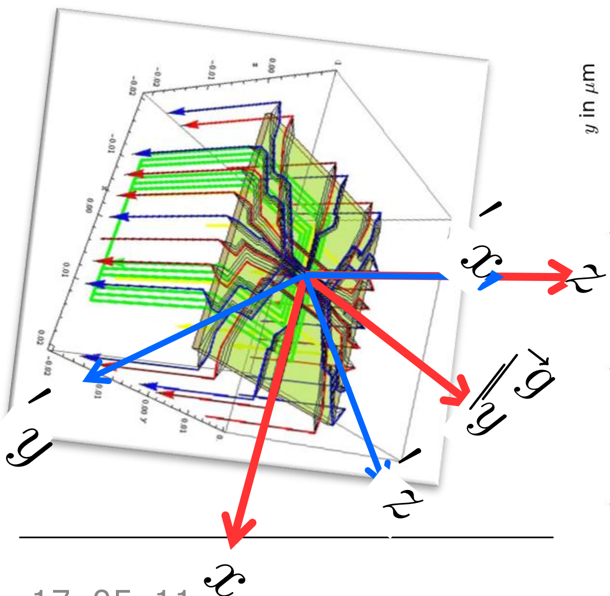

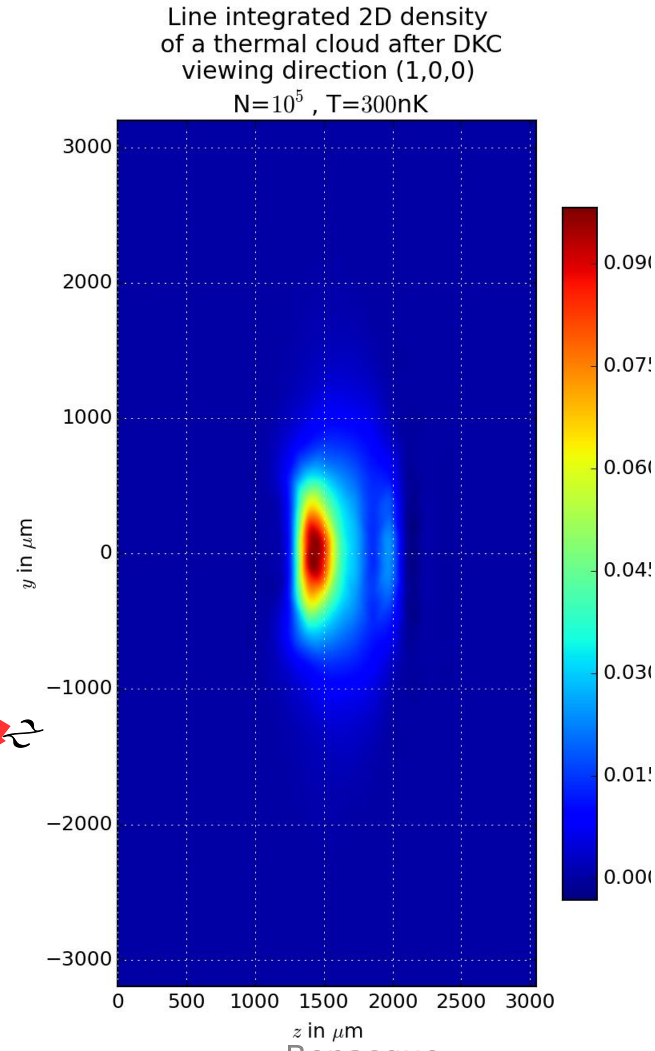

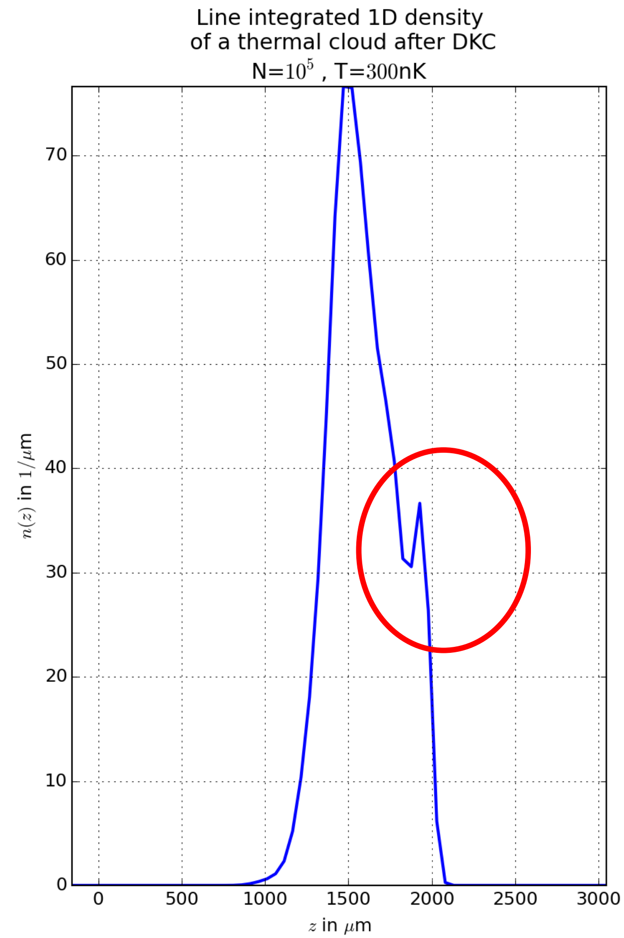

Coherent density of BEC $n^{(2)}(y, z, t_f)$

BEC: 3D time-dependent GP solution
2D column integrated densities
a) 0 ms, b) 150 ms,
c) 300 ms, d) 450 ms
after lens

N=10^5 particles

Scaling sizes:

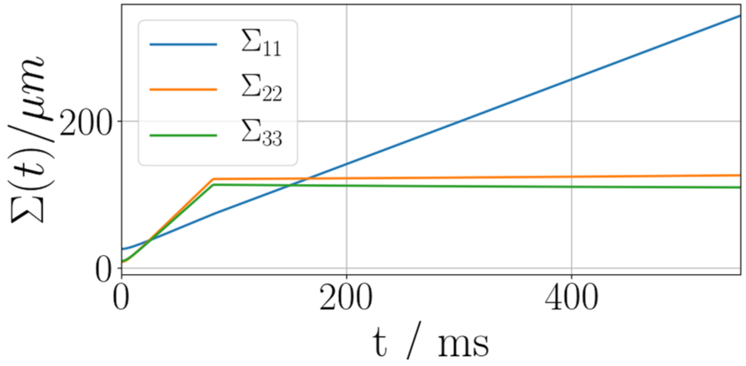

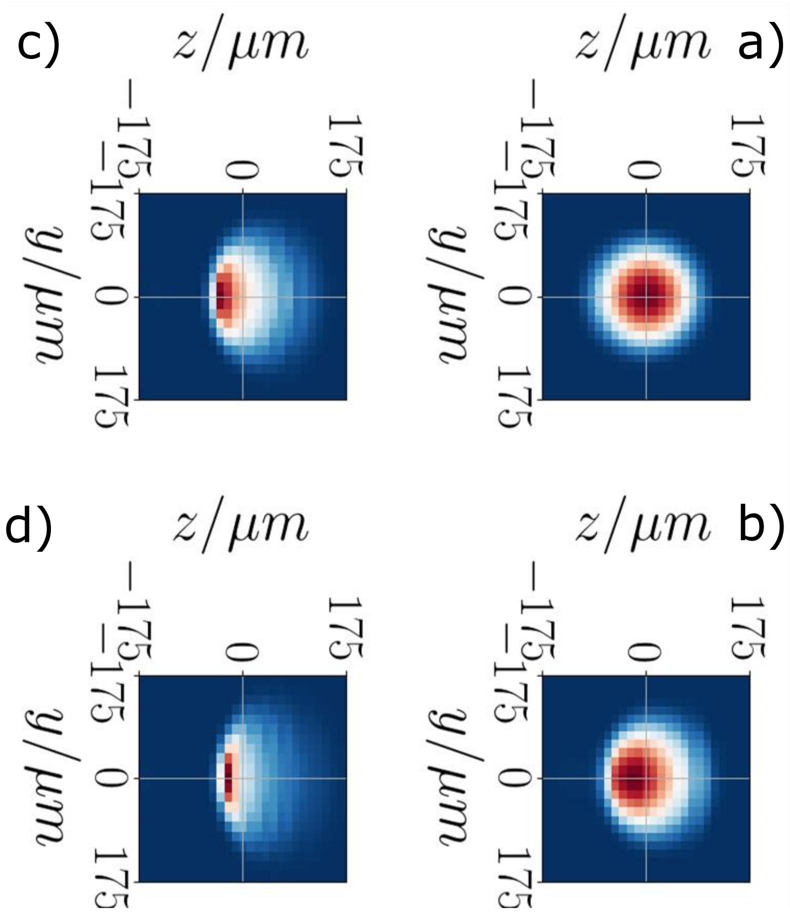

Application 2: Thermal Mach Zehnder-Interferometer

-thermal matter wave optics
M. Schneider

Mach-Zehnder interferometer

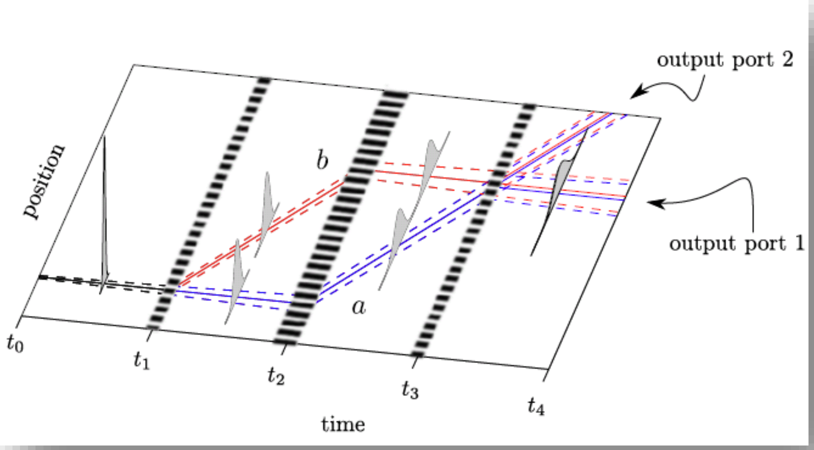

Gravity: population oscillation, acceleration sensor

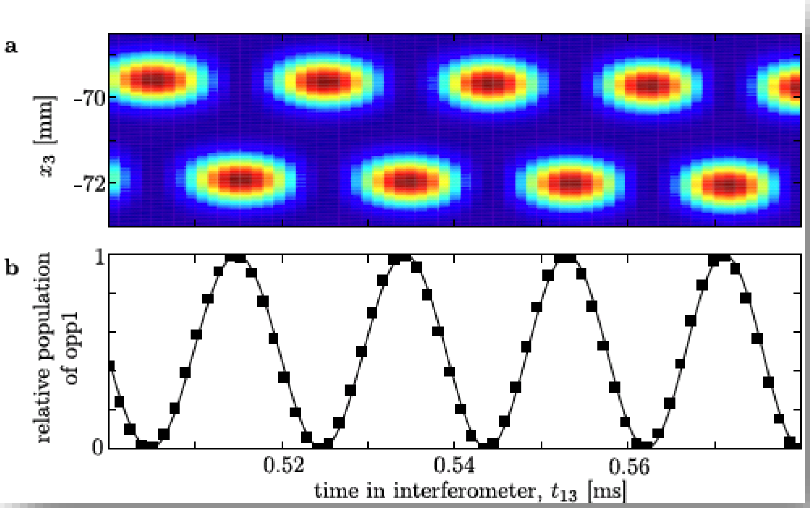

Ray-tracing with matter waves

TECHNISCHE UNIVERSITÄT DARMSTADT

Simulation of interferometry with
classical transport & coherence creating devices

Wigner function: a quantum distribution in phase space

$$f(x,p) = \int_{-\infty}^{\infty} d\xi \, \frac{e^{-ip\xi/\hbar}}{2\pi\hbar} \langle x + \tfrac{\xi}{2} | \hat{\rho} | x - \tfrac{\xi}{2} \rangle$$

Coherent squeezed state

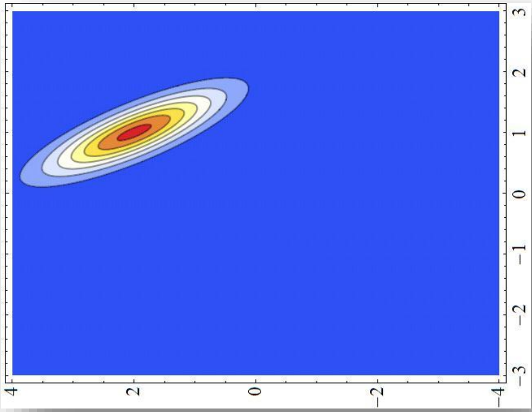

Number state n=6

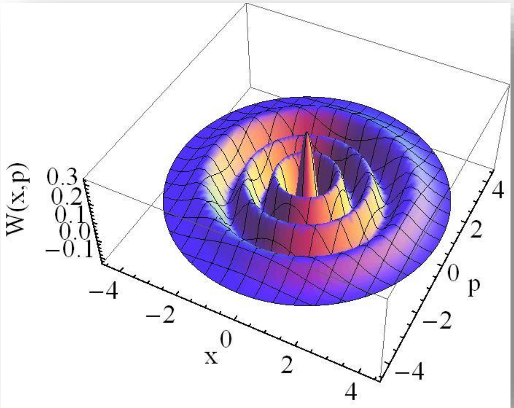

Classical transport in phase space

TECHNISCHE UNIVERSITÄT DARMSTADT

Transport: Hamiltonian evolution in phase space

$$\frac{\partial f}{\partial t} - \{\mathcal{H}, f\} = 0, \qquad \text{if } \frac{\partial^l \mathcal{H}}{\partial x^l} = 0 \text{ for } l > 2 \text{ and odd}$$

Free expansion

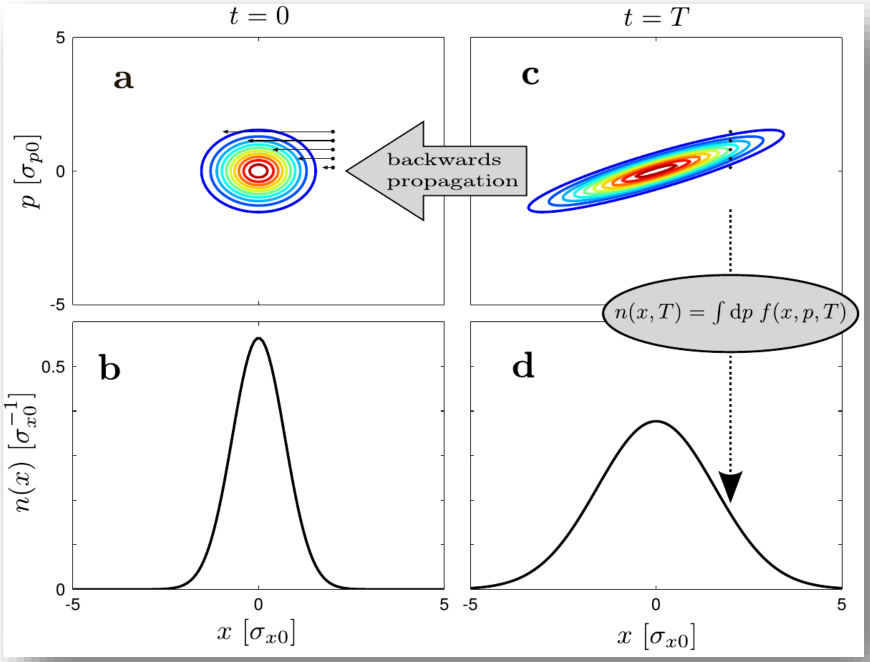

Harmonic lens

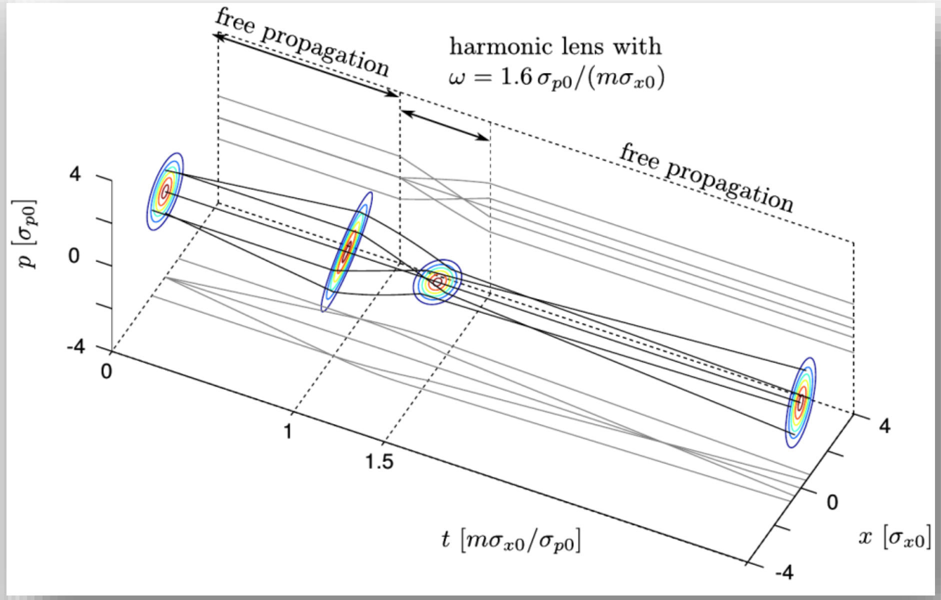

Coherence creating devices

- **Double slits** or **beam-splitters** in Hilbert-space
- **E.g.: Bragg scattering,** laser beam splits matter wave in coherent superposition, creation of coherence

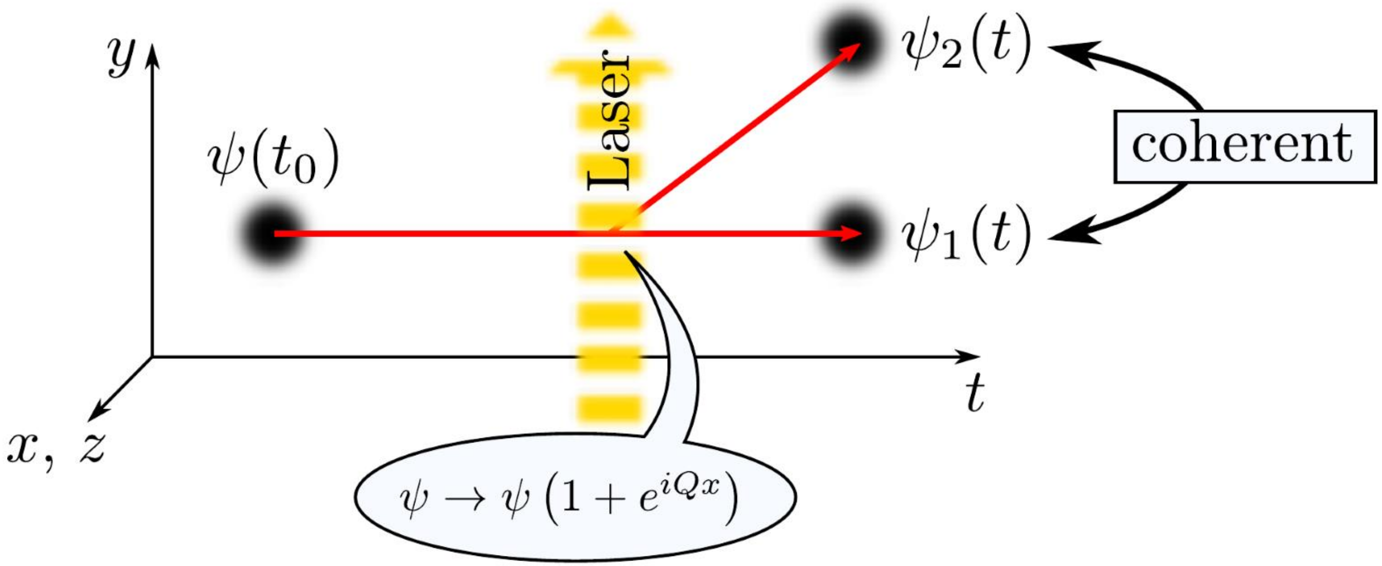

NOT described by classical transport

Beam-splitter in phase-space

Wigner function
in phase space

Before
and
after
a beam splitter

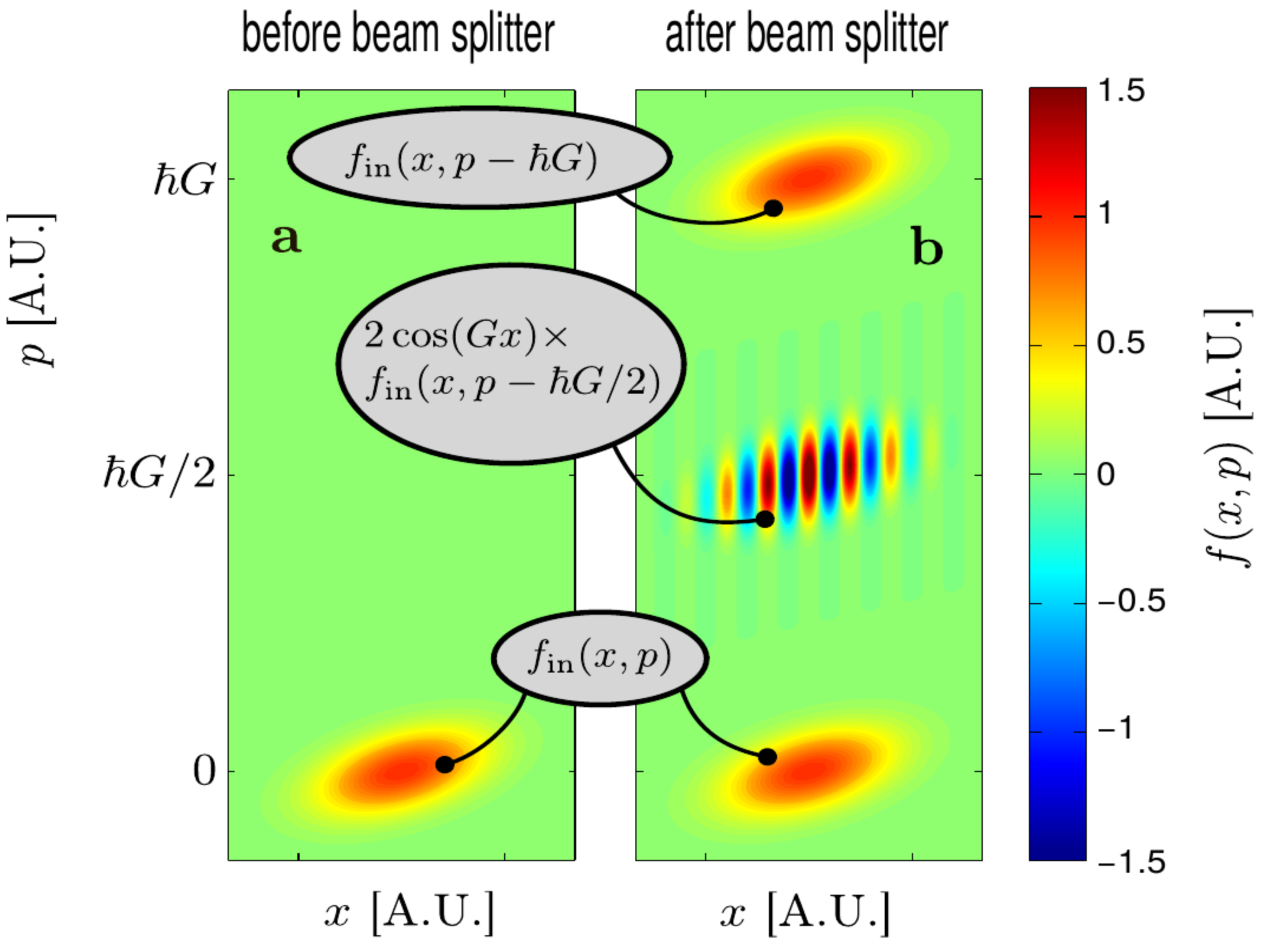

Mach-Zehnder interferometer

MZ interferometer in time MZI sequence in phase-space

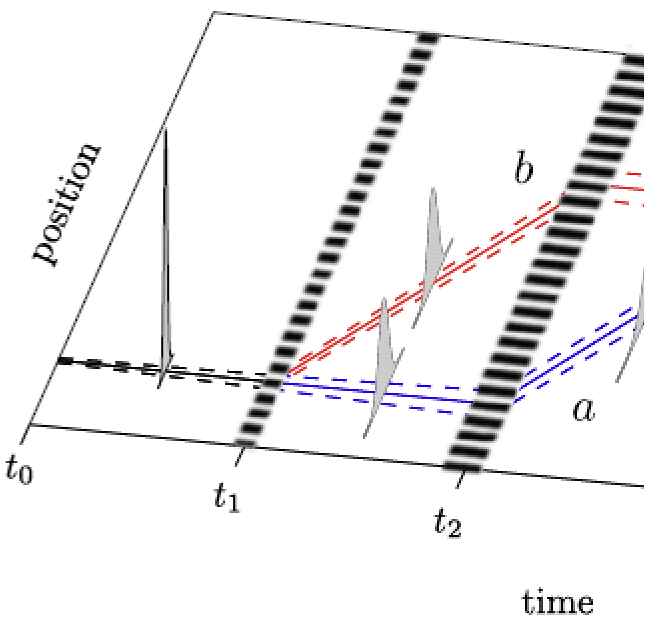

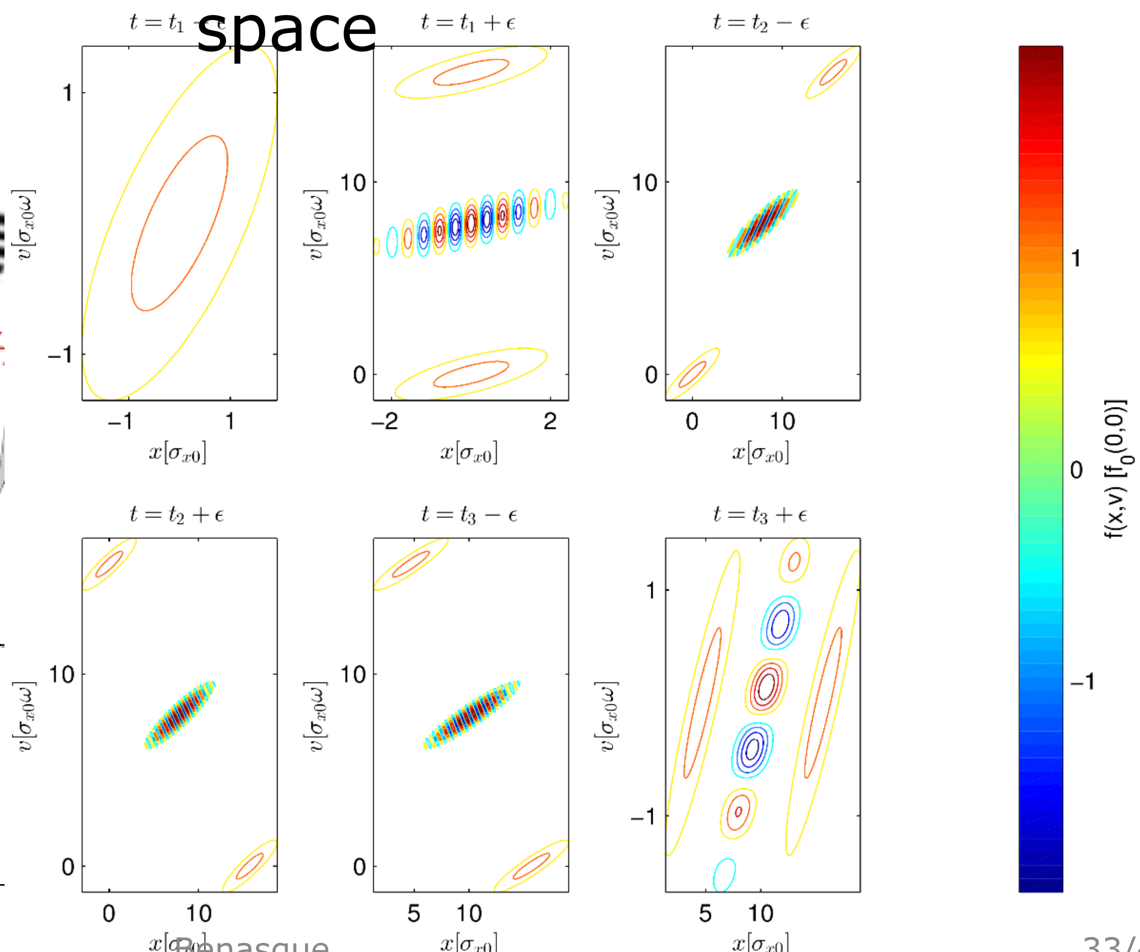

Free space: 3D asymmetric MZI

Temperature dependence:

2D density plots
1D cross sections
and
Fourier transforms
for three different temperatures:
T=100nk
T=500nk
T=1000nk
after recombination

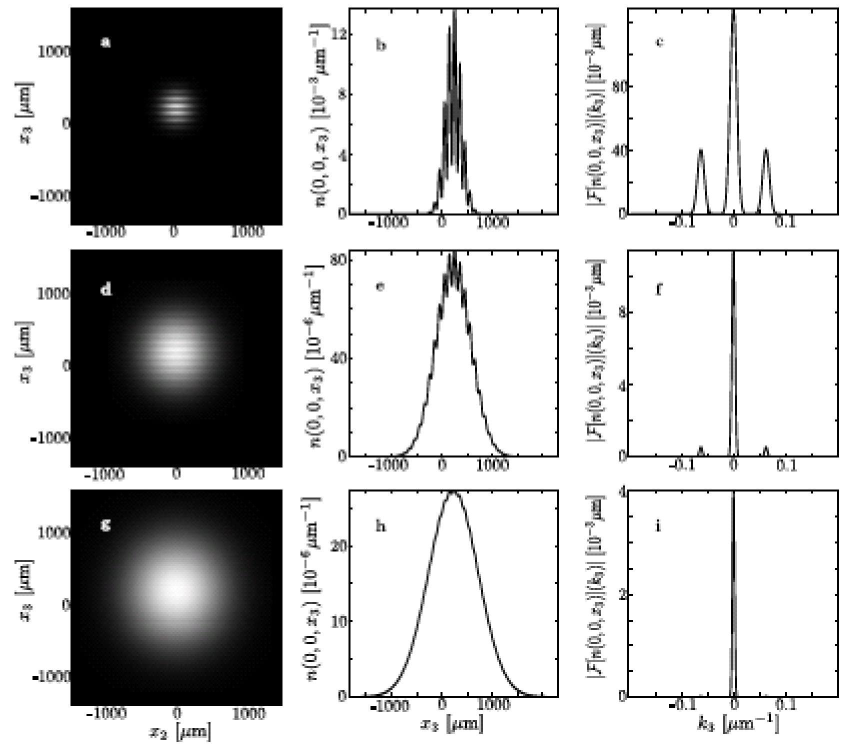

Figure 7.5.: Position densities after passing a MZI for various temperatures of the initial state. These are $T = 100$nK (1st line, **a**, **b**, **c**), $T = 500$nK (2nd line, **d**, **e**, **f**), and $T = 1000$nK (3rd line, **g**, **h**, **i**). The left column (parts **a**, **d**, **g**) shows 2D slices in the x_2-x_3-plane with x_1=0 of the 3D density. The middle column (parts **b**, **e**, **h**) displays the densities along the x_3 axis with $x_1 = x_2 = 0$. The right column (parts **c**, **f** ,**i**) shows the absolute values of Fourier transforms of densities along the x_3 axis, depicted in the middle columns. Initial state parameters are $(\omega_1, \omega_2, \omega_3) = 2\pi(127.3,\ 127.3,\ 31.8)$Hz, M = 87amu, $N = 10^5$. MZI parameters are $t_{01} = 20$ms, $t_{12} = 10$ms, $t_{23} = 9.9$ms, $t_{34} = 10$ms, $\mathbf{G} = (0,\ 0,\ 31.42)\mu\text{m}^{-1}$.

Free space: 3D asymmetric MZI

Time dependence

2D density plots
1D cross sections
and
Fourier transforms
@ T=100nk for three different times after recombination

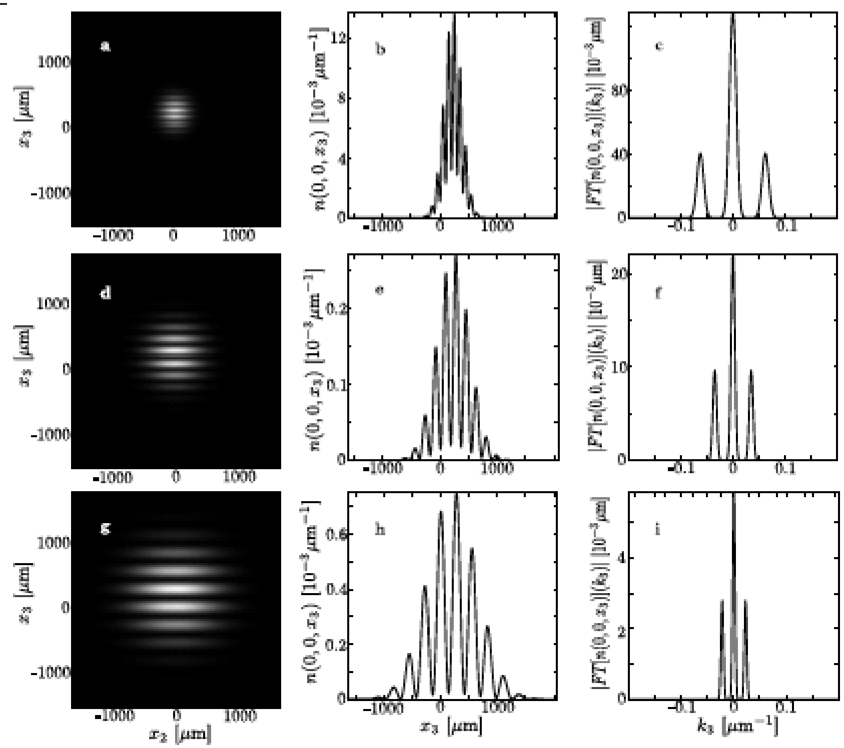

Figure 7.6.: Position densities after passing a MZI for various timespans between recombination and detection, t_{34}. These are $t_{34} = 10$ms (1st line, **a**, **b** ,**c**), $t_{34} = 50$ms (2nd line, **d**, **e** ,**f**), and $t_{34} = 100$ms (3rd line, **g**, **h** ,**i**). The left column (parts **a**, **d**, **g**) shows 2D slices in the x_2-x_3-plane with x_1=0 of the 3D density. The middle column (parts **b**, **e**, **h**) displays the density along the x_3 axis with $x_1 = x_2 = 0$. The right column (parts **c**, **f** ,**i**) shows the absolute value of the Fourier transform of the density along the x_3 axis, depicted in the middle columns. Initial state parameters are $(\omega_1, \omega_2, \omega_3) = 2\pi(127.3,\ 127.3,\ 31.8)$Hz, $M = 87$amu, $T = 100$nK, $N = 10^5$. MZI parameters are $t_{01} = 20$ms, $t_{12} = 10$ms, $t_{23} = 9.9$ms, $\mathbf{G} = (0,\ 0,\ 31.42)\mu m^{-1}$.

Fringe contrast= relative strength of Fourier components

MZI in gravity

Real space MZI sequence

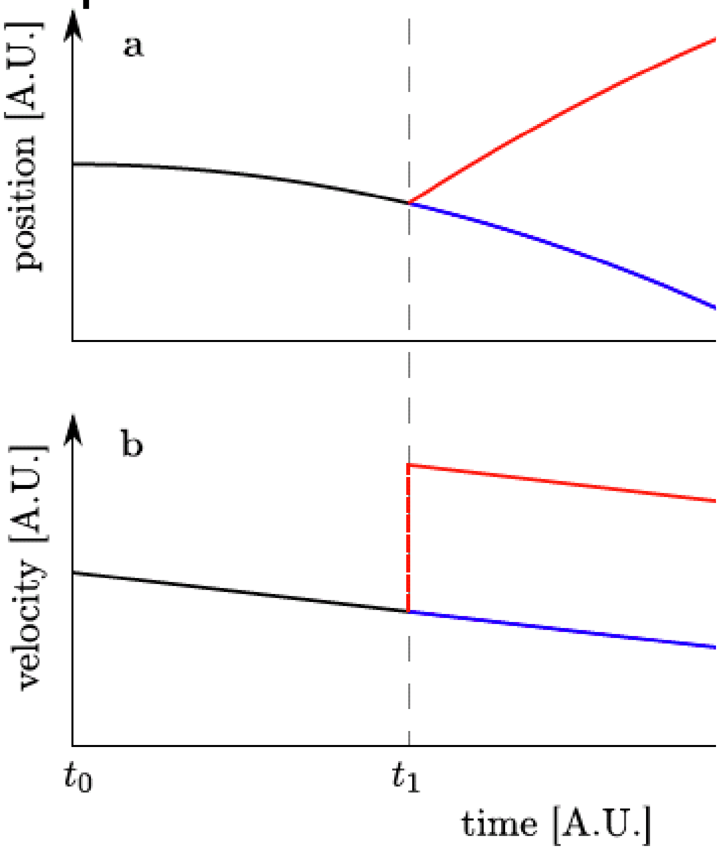

MZI in phase space

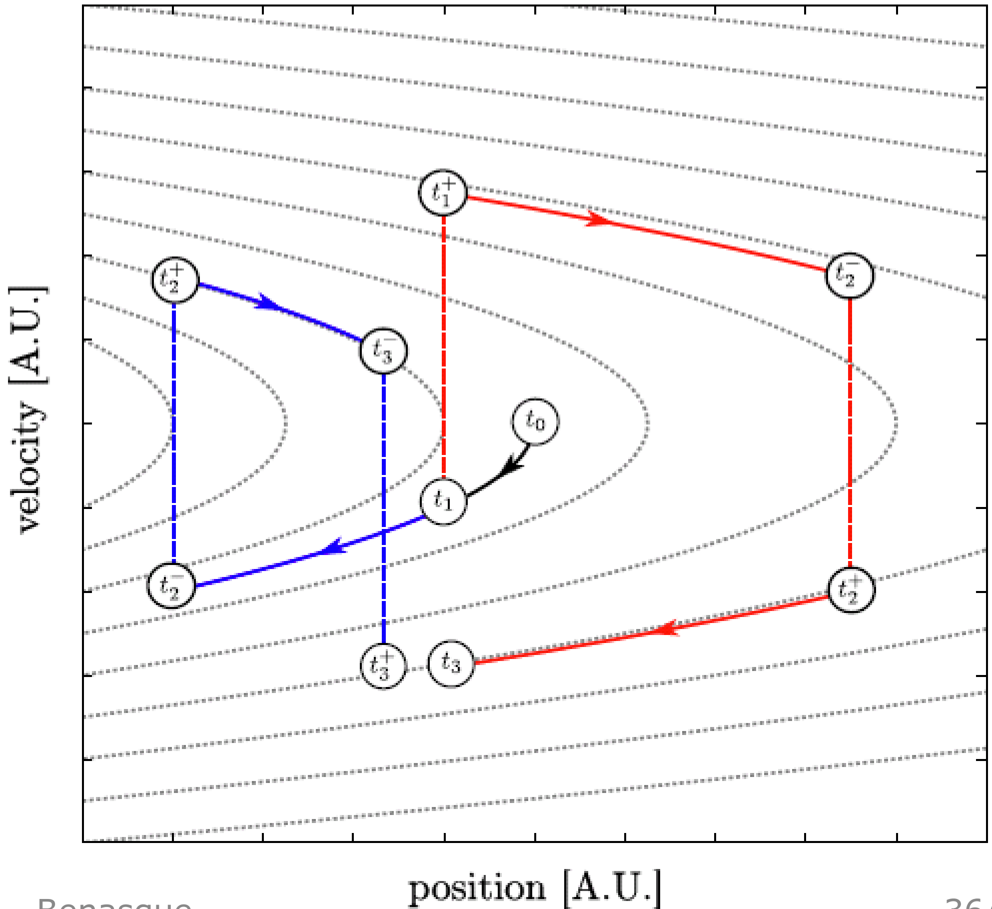

Acceleration sensor for gravity

Symmetric MZI

Population oscillations between the **two output ports 1+2** of a symmetric MZI (t23=t12)

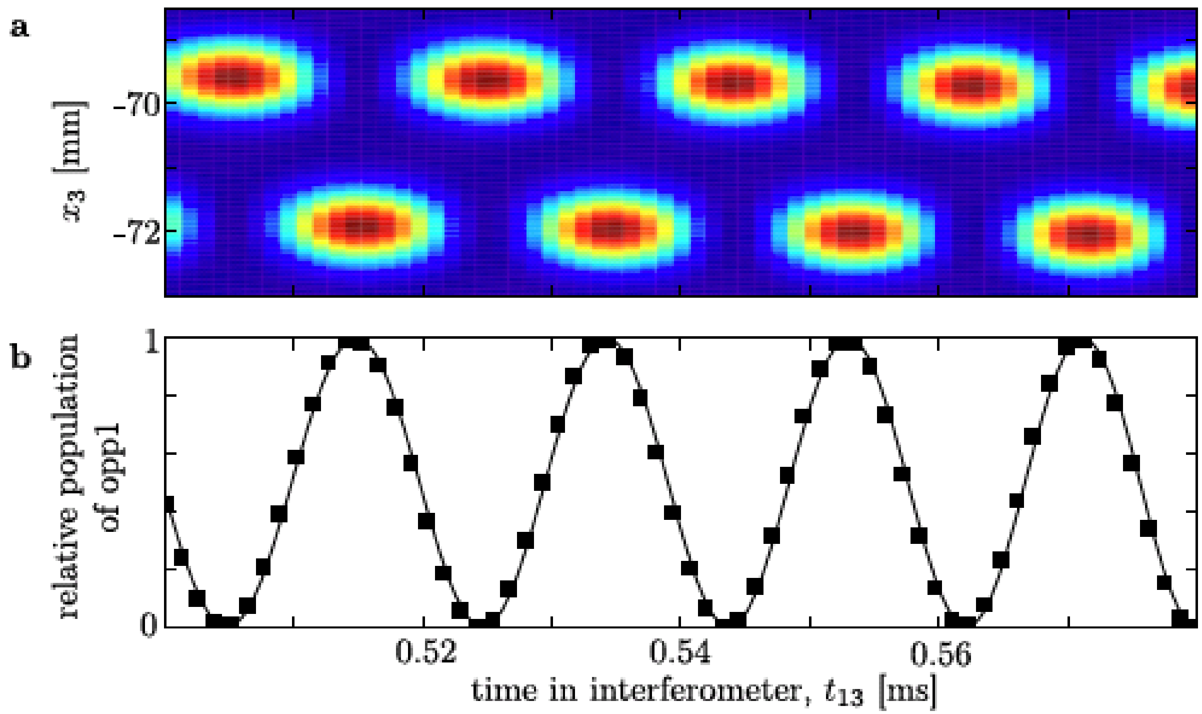

Figure 7.8.: Population of output ports under influence of constant gravity acceleration $\ddot{x}_3 = -g = 9.81\mu\mathrm{m/ms}^2$. Part **a**: False color representation of position density along vertical direction x_3. Part **b**: Relative population of output port 1. Other parameters are $t_{01} = 20\mathrm{ms}$, $t_{34} = 100\mathrm{ms}$, $N = 10^5$, $M = 87\mathrm{amu}$, $T = 100\mathrm{nK}$, $G = 31.42\mu\mathrm{m}^{-1}$. Initial trap is harmonic with $(\omega_1, \omega_2, \omega_3) = 2\pi(127.3,\ 127.3,\ 31.8)\mathrm{Hz}$.

Application 3: Coupled Josephson-rings

-quantum mw-optics
M. Sturm

Bose-Hubbard system: M=12 sites, N=4 particles, onsite interation U, intraring hopping J, interring hopping K<<J

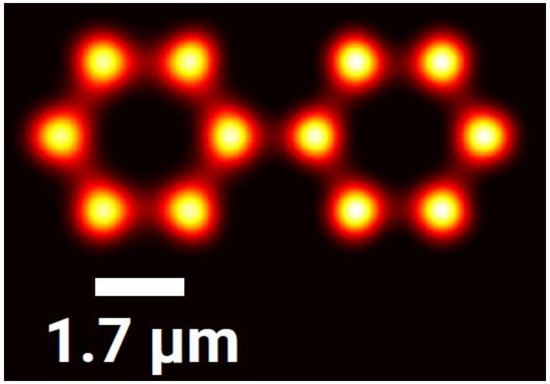

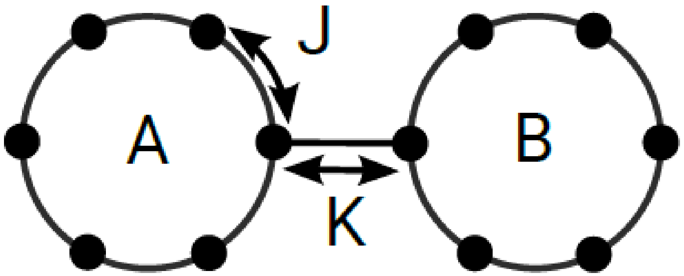

$$\hat{H} = \hat{H}_A + \hat{H}_B - K(\hat{a}_0^\dagger \hat{b}_0 + \hat{b}_0^\dagger \hat{a}_0) \qquad \hat{H}_A = \frac{U}{2}\sum_{i=1}^{M} \hat{a}_i^\dagger \hat{a}_i^\dagger \hat{a}_i \hat{a}_i - J \sum_{\langle ij \rangle} \hat{a}_i^\dagger \hat{a}_j$$

Tunneling dynamics

TECHNISCHE UNIVERSITÄT DARMSTADT

- **Initial state:** all atoms in ground-state of ring A
- **No interaction:** sinusoidal J-oscillations

$$\tau_J = h\frac{M}{K}$$

- **Weak interactions:** collapse and revival

$$\tau_C = \tau_R\sqrt{\frac{2}{\pi^2(N-1)}} \quad \tau_R = \frac{M}{U}$$

- **Strong interactions:** self-trapping, many-body tunneling resonances

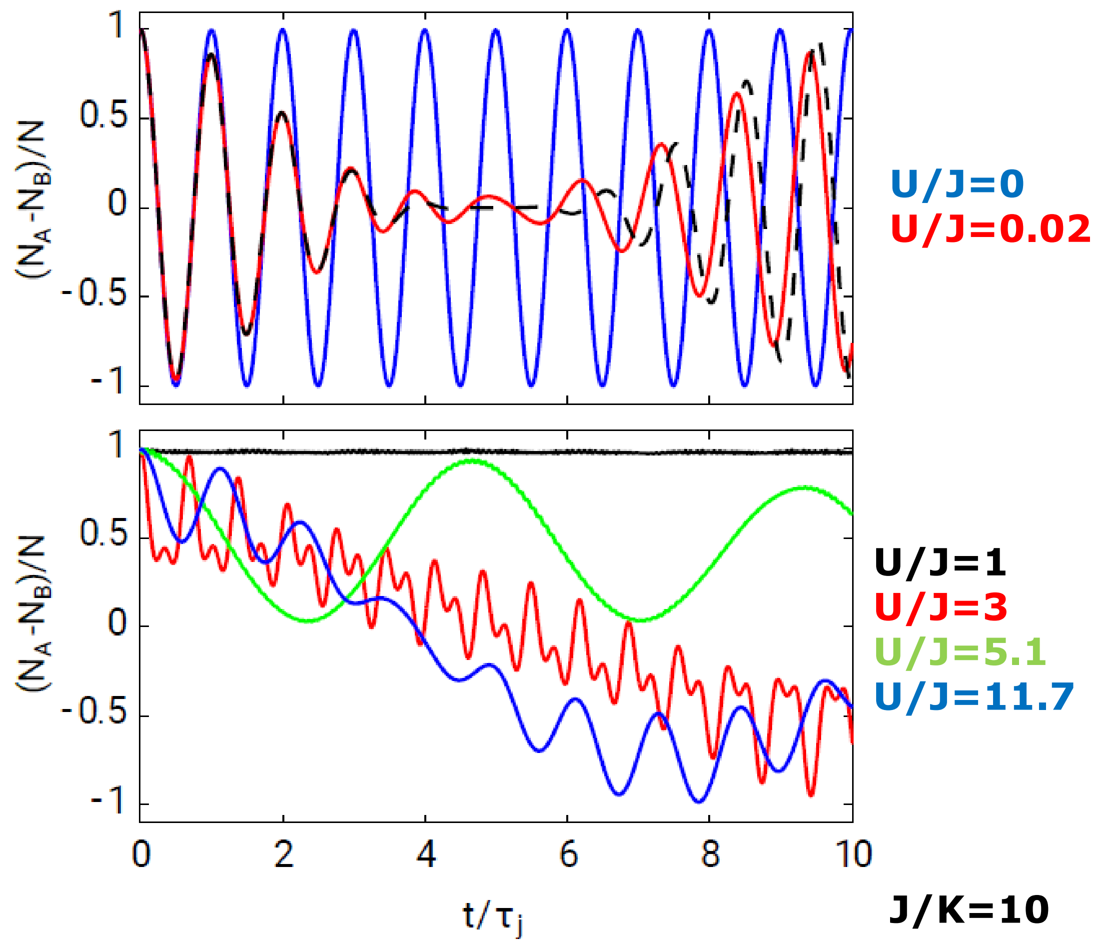

Many-body resonances

- Minimal population inversion

$$\zeta_m = \min_{0\leq t\leq\tau} \frac{N_A - N_B}{N}$$

- Resonances explained by level crossing of mb-states of isolated rings

$$|N_A, q_A\rangle_A \otimes |N_B, q_B\rangle_B$$

- Similar effects: tilted 1D lattices F.Meinert et al., PRL **116** 205301 (2016)
  double-wells Juliá-Díaz et al. PRA **82** 063626 (2010)

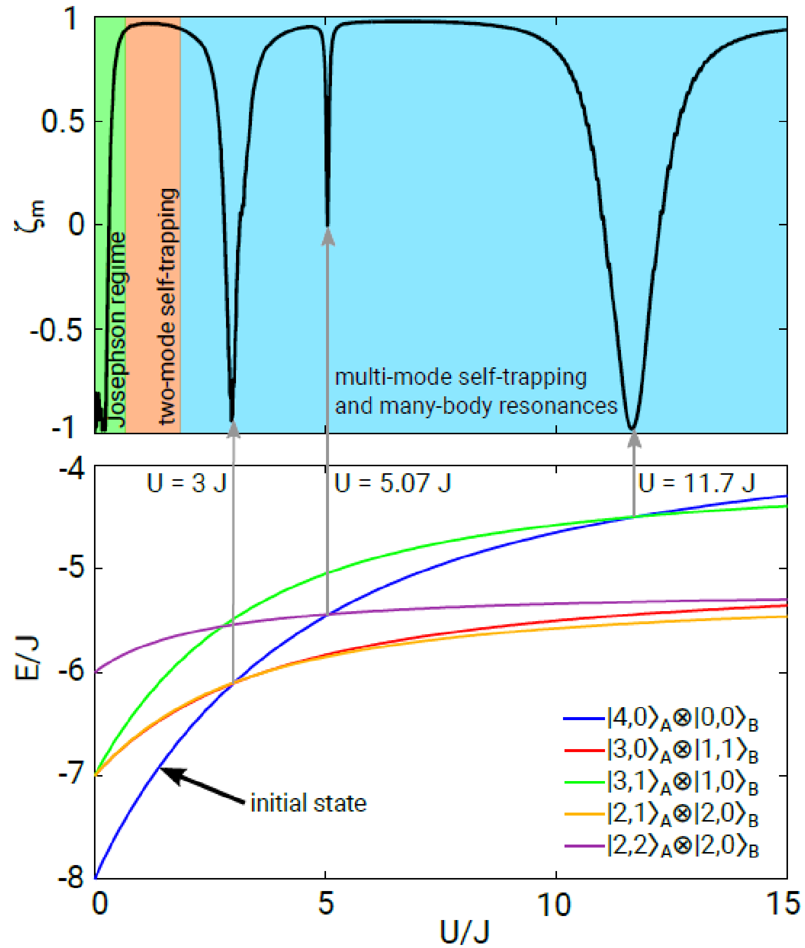

Summary: technical mw-optics

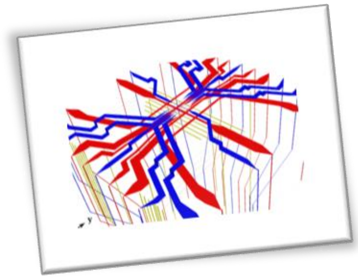

Software → hard ware → space

Toolbox mw-optics

a. Magnetic traps & lenses
b. Designing quantum simulators with micro lenses (M. Sturm, M. Schlosser, G. Birkl)
c. Bragg beam-splitters

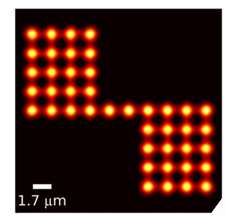

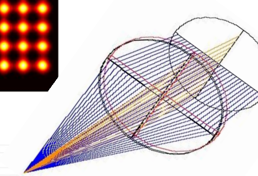

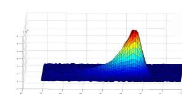

Methods & applications

a. geometical mw-optics: raytracing, aberrations
b. thermal mw-optics: 3D interferometry @ finite T
c. coherent mw-optics: 2 s, delta-kick-collimation
d. quantum mw-optics: JJ's manybody resonances

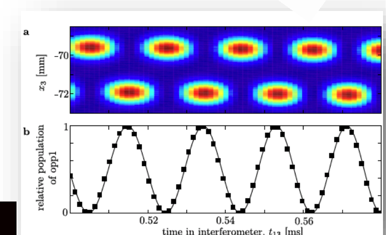

Thank you for the attention!